PERMANENT MAGNETS

Permanent magnets have been known since classical antiquity. Lodestones, rare rocks composed mainly of iron oxide that may have been naturally magnetized by lightning strikes, offered humans their first palpable demonstration of action at a distance, providing a stable magnetic field that could be manipulated by the owner of the magnetic stone. The counterintuitive attraction of iron to the magnet delights children, and archetypical but quite obsolete images of bright red horseshoe magnets continue to adorn science texts for primary schools.

Modern permanent magnets are highly sophisticated products of a union between physics and metallurgy. Their ferromagnetic properties are most simply characterized by the maximum energy product, a figure of merit proportional to the energy in kilojoules per cubic meter (kJ/m^3) stored in the magnetic field created by a given volume of magnetic material. The energy product increased exponentially during the twentieth century, doubling roughly every 12 years (Fig. 1). The laboratory record of 450 kJ/m^3, is held by a neodymium–iron–boron alloy. Neodymium is one of the rare-earth elements that can be alloyed with iron or cobalt to produce materials with outstanding magnetic properties. Many consumer electronic devices—portable computers and telephones, personal stereos, and cordless tools—would not exist without rare-earth magnets, which date from the late 1960s. Cheaper ferrite magnets are very widely used for holding applications and small dc motors.

Myths concerning the origins of magnetism can be found on four continents, in ancient Greece, Egypt, China, and Guatemala, but it was in China in the centuries preceding our era that a protoscience of magnetism developed in the context of arcane practices of geomancy and divination. By the Sung period (960 to 1279), technology for manufacturing steel wire for use as compass needles and magnetizing them with a lodestone or by cooling in the Earth's magnetic field was firmly established, both in China and in Europe. Adoption of the mariner's compass, the first practical permanent magnet device facilitated the great voyages of discovery that changed the face of the globe.

Modern understanding of magnetism began with the discovery by Oersted in 1820 of its relationship with electricity. This eventually led to the classical unification of electricity, magnetism, and light in Maxwell's equations. But only in the twentieth century was a satisfactory fundamental understanding of the phenomenon attained that incorporates elements of the two great achievements of modern physics: relativity and quantum mechanics. Permanent magnets generate a magnetic field with no need for any external power source, thanks to the perpetual quantized electric currents associated with spin and orbital motions of the electronic charges. All magnetism is related to electric currents; there are no elementary magnetic poles. The elementary quantity is the magnetic dipole $\boldsymbol{m}$, which is equivalent to a current loop; the magnetic dipole moment associated with the electron is the Bohr magneton, $\mu_B = 9.274 \times 10^{-24}\ A \cdot m^2$. The magnetization $\boldsymbol{M}$ of a solid is just the sum per unit volume of all the atomic magnetic moments associated with each atom's electrons. Units of $\boldsymbol{M}$ are amperes per meter.

Until the end of the nineteenth century, the only artificial magnets were weak and unstable, made of hard carbon steel. For a while following Oersted's discovery, steel magnets featured prominently in early manifestations of electrotechnology. Motors were built incorporating batteries of horseshoe magnets; generators were engineered around its elegant but bulky form. However, permanent magnets were soon replaced by the more compact and versatile electromagnets, resulting from the demonstration by Ampère and Arago that a magnet is equivalent to a current-carrying coil. This work, together with Faraday's principle of electromagnetic induction, led to the electrification of the planet. However, with the recent dramatic improvement in their magnetic properties (Fig. 1), permanent magnets are in turn replacing electromagnets in many small electrical machines and as a means of generating magnetic fields.

A uniformly magnetized state is rarely the most stable energetically because of the energy $\frac{1}{2} \int \mu_0 H^2 d\boldsymbol{r}$ stored in the magnetic field produced by the magnet in the surrounding space. This energy can be greatly reduced if the magnetization of the whole is split into a pattern of domains magnetized in different directions as suggested in Fig. 2. Only a slight energy penalty is incurred by the creation of domain walls, so the natural configuration of a piece of normal ferromagnetic material such as an iron wire is a multidomain state with no net magnetization. The art of making a permanent magnet is to achieve a microstructure in which the metastable fully magnetized state persists indefinitely because reverse domains are difficult to nucleate, or domain walls are pinned and cannot easily move to expand the regions of reverse magnetization.

A magnetic material is characterized by its hysteresis loop, which is a plot of the magnetic polarization $\boldsymbol{J}$, measured in teslas, as a function of the magnetic field $\boldsymbol{H}$, measured in amperes per meter, which acts upon the material. A typical loop is shown in Fig. 3. Polarization is simply related to magnetization by $\boldsymbol{J} = \mu_0 \boldsymbol{M}$, where μ_0 is the magnetic constant, $4\pi \times 10^{-7}\ T \cdot m/A$. The magnetic field $\boldsymbol{H}$ is the sum of any externally applied field $\boldsymbol{H}_{ext}$ and the field $\boldsymbol{H}_d$ created by the magnet itself:

$$\boldsymbol{H} = \boldsymbol{H}_{ext} + \boldsymbol{H}_d \qquad (1)$$

Saturation polarization J_s and remanent polarization J_r in zero field are defined from the hysteresis loop. The coercivity H_c is the magnitude of the reverse field acting on the magnet that will just reduce the net polarization to zero. The reverse field may be externally applied, but there will always be a contribution $\boldsymbol{H}_d$ of internal origin written as $-D\boldsymbol{M}$, where D is a numerical demagnetizing factor depending only on the sample shape, which ranges from 0 for a long rod to 1 for a flat plate. The inadequacy of steel magnets arises from their lack of coercivity. Since the magnetization of iron is 1710 kA/m but a typical coercivity for a steel magnet is 10 kA/m, it is really only possible to make them by the expedient of using a long needle or taking a long bar with a small value of D and bending it into a horseshoe shape.

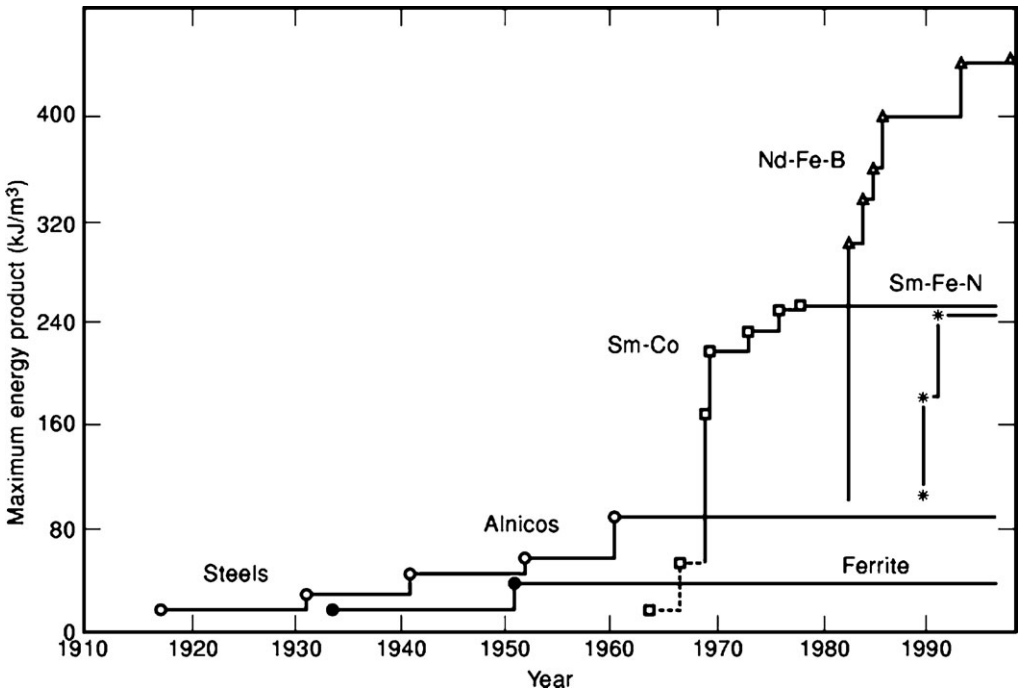

Figure 1. Progress in the maximum energy product $(BH)_{max}$ of permanent magnets during the twentieth century.

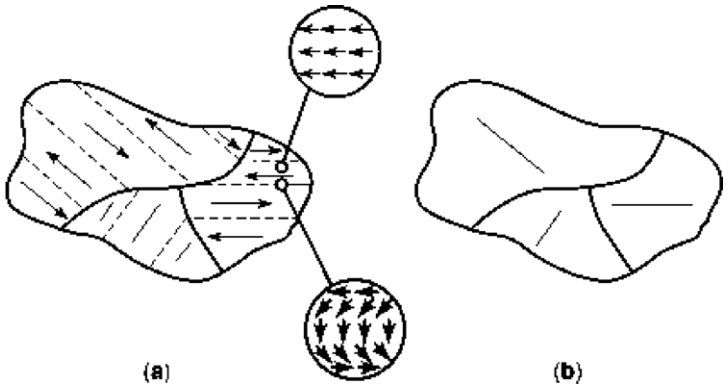

Figure 2. Polycrystalline ferromagnet (a) in the unpolarized state and (b) in the remanent state. Grain boundaries and domain walls are represented by solid and dotted lines, respectively. Long arrows parallel to the easy axes of the crystallites represent the polarization in each domain. The short arrows represent atomic magnetic moments.

Figure 4 shows $\boldsymbol{J}$ and $\boldsymbol{H}$ for a permanent magnet in the absence of any externally applied field. It is clear that $\boldsymbol{H}$ $(= \boldsymbol{H}_d)$ is oppositely directed to $\boldsymbol{J}$ within the magnet. The magnetizing process involves applying an external field $\boldsymbol{H}_{ext}$ sufficiently large to overcome $\boldsymbol{H}_d$ thereby saturating the polarization by eliminating the domain structure and aligning the moments (Fig. 3).

Magnet applications always involve delivering flux from the magnet into an adjacent region of space known as the air gap. In free space, the flux density $\boldsymbol{B}$ (also known as the induction) is simply $\mu_0\boldsymbol{H}$, but in the magnet itself the B field is quite different from the H field, as indicated in Fig. 4. The continuity of the normal component $B_\perp$ across the magnet surface follows from Maxwell's equation $\nabla \cdot \boldsymbol{B} = 0$. The three quantities are related by

$$\boldsymbol{B} = \mu_0\boldsymbol{H} + \boldsymbol{J} \qquad (2)$$

Engineers often consider the $B:H$ loop, rather than the $J:H$ loop. The coercivity ${}_BH_c$ on the $B:H$ loop is smaller than H_c, but the remanence is the same, $B_r = J_r$. The maximum energy product, denoted by the symbol $(BH)_{max}$, has a simple interpretation: it is the area of the largest rectangle that can be inserted in the second quadrant of the BH loop, as shown in Fig. 5. In the absence of an external field $\boldsymbol{H}_{ext}$, the magnet is subject to its own demagnetizing field $\boldsymbol{H}_d$, and the working point is a point on the second quadrant of the hysteresis curve that depends only on the magnet shape. Permanent or "hard" magnetic materials must therefore have broad hysteresis loops, with $\mu_0 H_c > J_r/2$. Limits on the energy product available from any given material can be deduced from the ideal situation of a perfectly rectangular $J:H$ loop; they are $(BH)_{max} < J_r^2/4\mu_0$ and $(BH)_{max} < J_r\ {}_BH_c/2$, when the coercivity is low. Hence it is desirable to increase the coercivity so that ${}_BH_c > J_r/2$ and have as large a polarization as possible.

The improvement of the energy-product value in the twentieth century was due to the introduction of new families of magnetic materials. The discovery of cobalt magnet steels in Japan in the early part of the century led to the

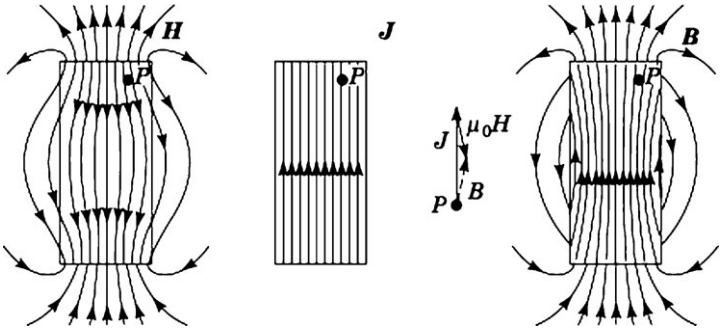

Figure 4. Illustration of $\boldsymbol{J}$, $\boldsymbol{H}$, and $\boldsymbol{B}$ due to a permanent magnet.

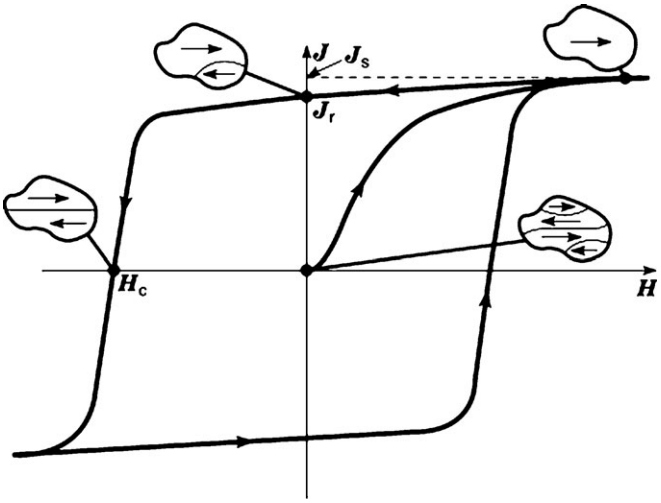

Figure 3. $J:H$ hysteresis loop for a permanent magnet. The initial magnetization curve from the thermally demagnetized state starts at the origin. Remanent polarization, saturation polarization, and coercivity are indicated as J_r, J_s, and H_c, respectively.

development of a family of iron–aluminium–nickel–cobalt alloys—the Alnico magnets—some of which are still in use today, especially in applications where the magnet

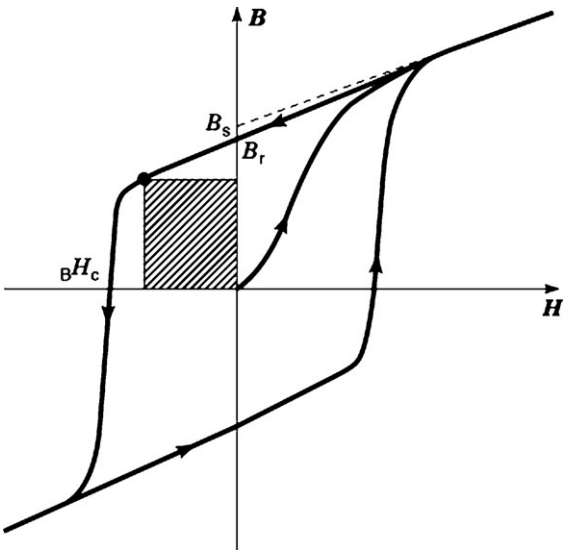

Figure 5. $\boldsymbol{B}:\boldsymbol{H}$ hysteresis loop for a permanent magnet. The energy product is the area of the shaded rectangle.

must withstand high temperatures up to 500°C. Ferromagnetism in any given material breaks down above a temperature T_C known as its Curie point. The maximum practical operating temperature of a permanent magnet is well below T_C. Cobalt-based alloys tend to have higher Curie points than iron-based alloys, and the high Curie points of Alnico magnets ($T_C \approx 800$°C) allow high operating temperatures.

The next advance came in the early 1950s with the development in the Netherlands of synthetic hexagonal ferrites. Like lodestone, these magnets are composed of an iron oxide ($BaFe_{12}O_{19}$ or $SrFe_{12}O_{19}$). Although they have never held the record energy product on account of their low saturation polarization J_s = 0.48 T, they are cheap, effective, and reliable. Ferrites today account for 90% of the mass and over half the value of all magnets produced worldwide, an annual market worth roughly US $6 billion in 2006, which is growing at more than 10% each year.

The other half of the market is mostly accounted for by rare-earth magnets having energy products 10 times greater than ferrites. These may be iron- or cobalt-based, but the most common involve the $Nd_2Fe_{14}B$ phase and account for well over a third of the total permanent magnet market. The pie chart in Fig. 6 shows the breakdown among the main magnet types. Rare-earth magnets are compact, top-of-the-range magnetic flux sources. Both rare-earth magnets and ferrites can have coercivities that exceed their magnetization, so magnets may be made in any shape. Squat cylinders with D = ½ are typical. Table 1 lists characteristics of typical commercial magnets.

The flux delivered to the air gap may be homogeneous or inhomogeneous, steady, or time varying. Permanent-magnet applications can be classified in several ways. One scheme uses the physical effect that is being exploited—torque on a magnet in an external field, force on a magnet or on a piece of soft magnetic material in a nonuniform field, force on a current-carrying conductor or on charged particles moving in a magnetic field, induced EMF, Zeeman splitting of energy levels, etc. A simpler scheme focuses on the characteristics of the magnet, distinguishing between static applications where the magnet exists to produce a steady magnetic field in some region of space, where what goes on has little effect on the flux density in the magnet itself, and dynamic applications where the working point shifts along the $B:H$ curve during operation. A list of typical examples of magnet applications is given in Table 2.

As the energy product increase the permanent magnet devices become smaller and lighter. A trend towards

Table 1. Characteristics of Typical Oriented Magnets

	B_r (T)	J_S (T)	H_C (kA/m)	$_BH_c$ (kA/m)	$(BH)_{max}$ (kJ/m^3)
$SrFe_{12}O_{19}$	0.41	0.47	275	265	34
Alnico	1.25	1.40	54	52	43
$SmCo_5$	0.88	0.95	1700	660	150
Sm_2Co_{17}[a]	1.08	1.15	800	800	200
$Nd_2Fe_{14}B$	1.28	1.54	1000	900	300

[a] Intergrown with 1:5 phase.

Table 2. Summary of Permanent Magnet Applications

Field	Magnetic Effect	Type	Examples
Homogeneous	Zeeman splitting	Static	Magnetic resonance impaging
	torque, Hall effect,	Static	Alignment of magnetic powder
	magnetoresistance	Static	Sensors, read-heads
	force on conductor,	Dynamic	Motors, actuators, loudspeakers
	induced emf.	Dynamic	Generators, microphones
Inhomogeneous	Force on charged particles;	Static	Beam control, radiation sources (microwave, UV, X ray)
	force on magnet;	Dynamic	Bearings, couplings, Maglev
	force on paramagnet	Dynamic	Mineral separation
Time-varying	Varying field	Dynamic	Magnetometers
	Force on iron	Dynamic	Switchable clamps, holding magnets
	Eddy currents	Dynamic	Metal separation, brakes

Table 3. Intrinsic Magnetic Properties of Phases Used in Permanent Magnet Manufacture

Compound		T_C(°C)	A_{ex}(pJ/m)	M_s(MA/m)	J_S(T)	K_1(MJ/m^3)	H_a(MA/m)	δ_W(nm)	γ_W(mJ/m^2)	d_c(μm)	$J_S^2/4\mu_0$(MJ/m^3)
$BaFe_{12}O_{19}$	hex.	470	6	0.37	0.47	0.25	1.1	15.4	5	0.68	44
$SmCo_5$	hex.	720	24	0.84	1.05	17	32	3.7	81	1.88	219
Sm_2Co_{17}	rhom.	827	25	1.03	1.30	3.3	5.1	8.6	36	0.49	336
$Nd_2Fe_{14}B$	tet.	312	9	1.28	1.61	4.9	6.1	4.2	27	0.24	516
$Sm_2Fe_{17}N_3$	rhom.	476	12	1.23	1.54	8.6	11.2	3.6	42	0.41	472

Table 4. Magnetization and Energy Product of Oriented and Isotropic, Sintered, and Bonded $SrFe_{12}O_{19}$ Magnets

$SrFe_{12}O_{19}$	M_r (MA/m)	$(BH)_{max}$ (kJ/m^3)
Intrinsic	0.38	45
Oriented sintered	0.33	34
Isotropic sintered	0.18	9
Oriented bonded	0.24	16
Isotropic bonded	0.14	5

Table 5. Temperature Coefficients and Maximum Operating Temperatures for Permanent Magnets

	T_C(°C)	dM_S/dT (%)	dH_C/dT (%)	T_{max}(°C)
$SrFe_{12}O_{19}$	450	−0.20	0.40	300
Alnico	880	−0.02	0.03	500
$SmCo_5$	720	−0.04	−0.20	250
Sm_2Co_{17}[1]	820	−0.03	−0.20	350
$Nd_2Fe_{14}B$	310	−0.13	−0.60	180

moving-magnet designs is coupled with miniaturization. Figure 7 illustrates how a radical design change has been envisioned from a fixed to a moving magnet in a dc motor or loudspeaker. The number of parts may be reduced, for example, by shifting the magnets of a brushless dc motor to the rotor and molding the magnets together with the shaft and gear in one piece. Moving magnets have low inertia, and the stationary windings can be thermally heat-sunk.

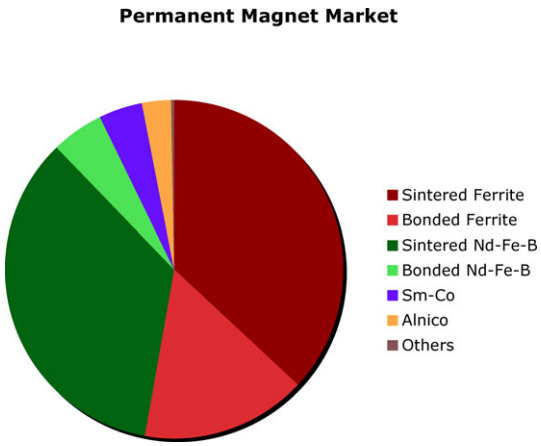

Figure 6. Breakdown of hard magnetic materials. The total market is roughly US $6 billion.

The advantage of the permanent magnet can be savored by comparing a small disk-shaped magnet with a coil having the same magnetic moment. A disk of diameter 8 mm and height 2 mm made of a material with $M = 1$ MA/m has $m \approx 0.1\ \mathrm{A \cdot m^2}$. An equivalent coil of the same diameter would need 2000 ampere-turns.

With respect to units, standard SI (International System) quantities and units are used here, with the convention preferred by engineers [Eq. (2)]. The obsolete electromagnetic cgs system is still encountered in the research literature. In that system, the magnetic moment is measured in *electromagnetic units* (emu). Equation (2) is replaced by $\boldsymbol{B} = \boldsymbol{H} + 4\pi\boldsymbol{M}$, where B is measured in gauss ($1\ \mathrm{G} = 10^{-4}\ \mathrm{T}$) and H is measured in oersteds ($1\ \mathrm{Oe} = 1000/4\pi\ \mathrm{A/m}$). $\mu_0 = 1$ G/Oe is generally omitted. M is often quoted in electromagnetic units per cubic centimeter. The energy product has units of megagauss-oersteds ($1\ \mathrm{MG \cdot Oe} = 100/4\pi\ \mathrm{kJ/m^3}$). Two other useful conversions are $1\ \mathrm{A \cdot m^2/kg} = 1$ emu/g and $1\ \mathrm{kA/m} = 1\ \mathrm{emu/cm^3}$).

MAGNETIC PROPERTIES

The basic requirements for a permanent magnet material are that it should be magnetically ordered with a Curie temperature well above room temperature and that it have a substantial polarization. Usually this means ferromagnetic order, and metallic magnets are generally based on the ferromagnetic elements iron or cobalt. There are few ferromagnetic oxides, but ternary iron oxides known as ferrites often order ferrimagnetically with two unequal antiparallel magnetic sublattices which yields a reduced net polarization compared to ferromagnetic order (Fig. 8).

A further requirement is that there should be a pronounced tendency for the magnetization to lie along a single axis or easy magnetic direction. This will favor hysteresis, since magnetic reversal then involves flipping the atomic moments through the maximum angle of 180°. The tendency towards an easy axis of magnetization is known as anisotropy. Easy-axis anisotropy is indispensi-

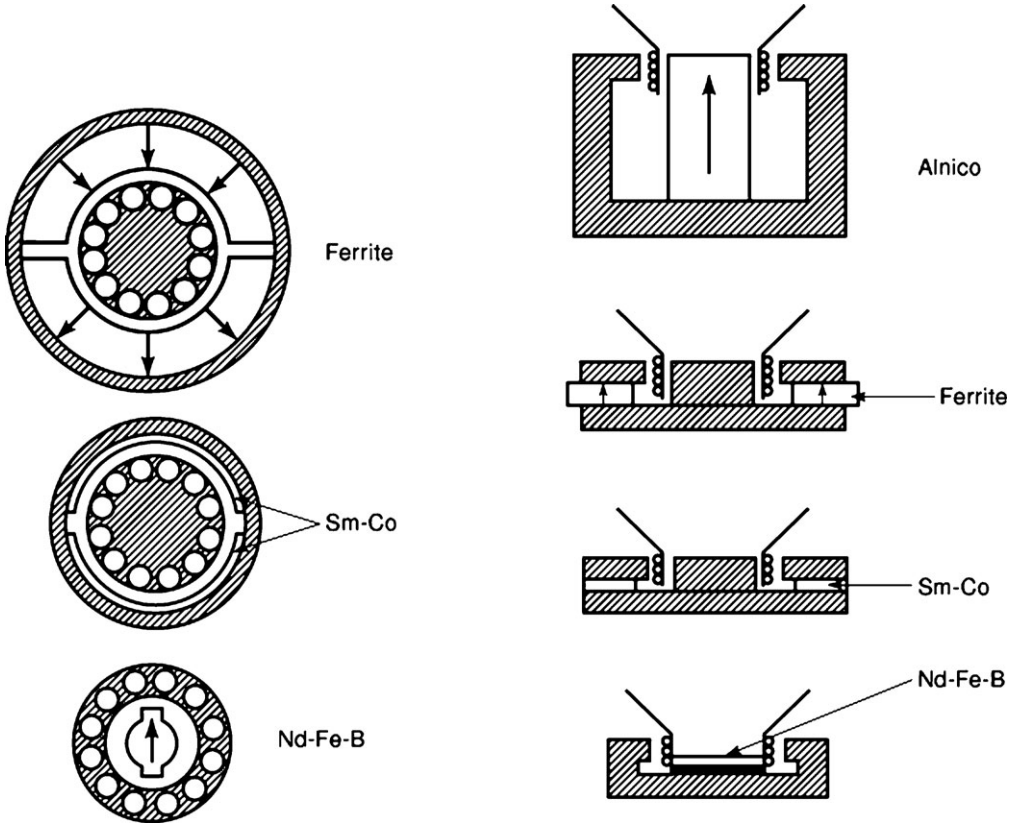

Figure 7. Illustration of the influence of improved magnets on the design of a dc motor and a loudspeaker. Soft iron is shaded.

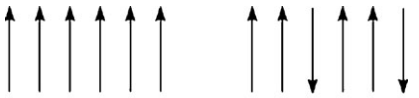

Figure 8. Magnetic order in (a) a ferromagnet and (b) a ferrimagnet. Each arrow represents the magnetic moment of an atom.

ble for maintaining the metastable domain configuration required of a permanent magnet. In most permanent magnets the anisotropy originates on an atomic scale through spin–orbit coupling of the electronic orbital states that are stabilized by the electrostatic field created at the atomic site by the rest of the crystal lattice. The atomic moment has corresponding preferred orientations or local easy directions in the crystal that reflect the point symmetry of the site. The macroscopic magnetocrystalline anisotropy obtained by summing all the single-ion contributions reflects the overall crystal symmetry. Hence the permanent magnet material should have a uniaxial crystal structure, usually rhombohedral, tetragonal, or hexagonal.

The anisotropy energy can be expressed as a series of terms involving the orientation (θ, ϕ) of the magnetization with respect to the crystal axes. In a tetragonal or hexagonal crystal the expression is, respectively,

$$K_a^{tet} = K_1 \sin^2\theta + K_2 \sin^4\theta + K_3 \sin^6\theta + K_2' \sin^4\theta \cos 4\phi + K_3' \sin^6\theta \cos 4\phi \quad (3a)$$

or

$$E_a^{hex} = K_1 \sin^2\theta + K_2 \sin^4\theta + K_3 \sin^6\theta + K_3' \sin^6\theta \cos 6\theta \quad (3b)$$

It is often sufficient to consider only the leading term

$$E_a = K_1 \sin^2\theta \quad (4)$$

which leads to an easy axis provided the first anisotropy constant K_1 is positive. Units of K_1 are joules per cubic meter.

Related to the anisotropy energy is the concept of the anisotropy field. The anisotropy is somehow equivalent to that produced by an effective field H_a acting along the easy direction. The analogy is useful, but inexact because the angular variation of magnetic energy in a field is $-\mu_0 M H_a \cos\theta$. The anisotropy field is defined as that needed to saturate the magnetization in a direction perpendicular to the easy axis. The orientation of the magnetization is given by the condition $dE/d\theta = 0$, so $\theta = \pi/2$ yields

$$H_a = 2(K_1 + 2K_2 + 3K_3)/J_s \quad (5)$$

When the higher anisotropy constants are neglected this reduces to

$$H_a = 2K_1/J_s \quad (6)$$

The anisotropy field sets an upper limit on the coercivity H_c; achievable coercivities are usually much less than H_a.

The role of rare-earth elements in alloys such as $Nd_2Fe_{14}B$ or $SmCo_5$ is to supply magnetocrystalline anisotropy. Elements in the first half of the 4*f* series, the light rare earths, are preferred because their exchange coupling with the ferromagnetic 3*d* elements leads to parallel alignment of 3*d* and 4*f* moments. Despite their name, crustal abundances of light rare-earths are similar to those of zinc or lead.

Another source of anisotropy that is exploited in Alnico magnets is shape anisotropy. These alloys are composed of needle-shaped nanoscale Fe–Co regions in an Al–Ni matrix (Fig. 9). The magnetization of a needle-shaped region tends to lie along the needle axis because the positive self-energy in the demagnetizing field $-\frac{1}{2}\boldsymbol{J}\cdot\boldsymbol{H}_d = \frac{1}{2}DM^2$ is thereby reduced. D is close to zero when the magnetization lies along the axis, but it is close to ½ in a perpendicular direction. In general, the values of D for the three perpendicular directions of a ellipsoid sum to 1. Equating the differences in energy between the hard- and easy-magnetization directions, $\theta = 0$ and $\pi/2$, to that given by Eq. (5) leads to a shape anisotropy constant

$$K_1^s = (1 - 3D)J_s^2/4\mu_0 \quad (7)$$

and a corresponding anisotropy field

$$H_a^s = (1 - 3D)J_s/2\mu_0 \quad (8)$$

The maximum theoretical coercivity achievable with shape anisotropy is therefore only $J_s/2\mu_0$, and it is difficult to obtain a value that comes close except in regions with nanoscale dimensions. There is no such limit on the anisotropy field due to magnetocrystalline anisotropy.

The atomic moments in a ferromagnet or ferrimagnet interact with each other by exchange interactions, which lead to the magnetically ordered state. The exchange energy is

$$E_{ex} = A_{ex}[\nabla|\boldsymbol{J}(\boldsymbol{r})/J_s|]^2 \quad (9)$$

where $\boldsymbol{J}(\boldsymbol{r})$ is the local magnetization vector and J_s is its magnitude. A_{ex} is measured in J/m; it is proportional to the Curie temperature T_C.

The magnetic state of the sample is therefore obtained by minimizing the total micromagnetic free energy

$$F = \int\{A_{ex}[\nabla|\boldsymbol{J}(\boldsymbol{r})/J_s|]^2 + K_1(\boldsymbol{r})\sin^2\theta(\boldsymbol{r}) + \cdots - \boldsymbol{J}_s\cdot(\boldsymbol{H}_d/2 + \boldsymbol{H}_{ext})\}\,d\boldsymbol{r} \quad (10)$$

where the four terms represent, respectively, the exchange energy, the anisotropy energy, the self-energy in the demagnetising field, and the Zeeman energy in the external field. In principle the hysteresis loop could be calculated by examining the energy landscape corresponding to the expression if $A(\boldsymbol{r})$ and $K_i(\boldsymbol{r})$ were known. In practice this is an impossible task, but solutions available in special cases provide important guidance to help understand the hysteresis in real magnets.

Domain Wall

Consider two domains in which the magnetization is oppositely directed along the easy magnetic direction (Fig. 10). Assuming the magnetization vector in the wall, known as a Bloch wall, rotates in a plane containing the easy axis of the two domains, the wall energy γ_w, in $J\cdot m^{-2}$, is obtained

Figure 9. Electron micrograph of an oriented Alnico magnet showing the distribution of fine magnetic needles (mainly FeCo) in a matrix (NiAl) that has a much smaller magnetic moment. (a) Plane of observation parallel to the preferred direction of magnetization. (b) The same, but perpendicular to the preferred direction. Magnification 50,000×.

by summing the exchange and anisotropy energies at each point:

$$\gamma_w = \int [A_{ex}(d\theta/dx)^2 + K_1 \sin^2\theta]dx \qquad (11)$$

This integral is minimized when the exchange and anisotropy terms are equal at every point across the wall, which leads to the domain-wall equations:

$$d\theta/dx = (K_1/A_{ex})^{1/2} \sin\theta \qquad (12a)$$

$$x = (A_{ex}/K_1)^{1/2} \ln[\tan(\theta/2)] \qquad (12b)$$

where x is the distance measured from the midpoint of the wall. Although the wall is infinite in extent in this continuum model, about 160° of the rotation occurs over a distance δ_w, known as the domain-wall width:

$$\delta_w = \pi(A_{ex}/K_1)^{1/2} \qquad (13)$$

The domain-wall energy evaluated from Eqs. (11) and (12) is

$$\gamma_w = 4(A_{ex}K_1)^{1/2} \qquad (14)$$

Typical values of A_{ex} and K_1 for rare-earth permanent magnets are 2×10^{-12} J · m^{-1} and 5×10^6 J · m^{-3}, respectively; hence $\delta_W \approx 1$ nm and $\gamma_w \approx 10^{-2}$ J · m^{-2}. Exact values for different compounds are given in Table 3.

Stoner-Wohlfarth Model

Here a small sample is considered and the magnetization reversal in a negative field is assumed to be coherent, so that the magnetization remains everywhere parallel to a direction making an angle ψ with the applied field. The energy is then

$$E = K_1 \sin^2\theta - \boldsymbol{J}_s \cdot (\boldsymbol{H}_d/2 + \boldsymbol{H}_{ext}) \qquad (15)$$

When the field is paralled to the easy magnetic direction and this is also the anisotropy axis,

$$H_c = 2K_1/J_s \qquad (16)$$

Note that K_1 may be due to magnetocrystalline anisotropy or shape anisotropy [Eq. (7)] or may include contributions from both. In the model, the coercivity is therefore equal to the anisotropy field. In the spirit of the model, coercivity is often expressed as

$$H_c = \alpha 2K_1/J_s + D_{eff}J_s/\mu_0 \qquad (17)$$

where α (<1) and D_{eff} and are empirical parameters determined from the temperature dependence of H_c, knowing the temperature dependence of K_1 and J_s.

Coherent rotation of the magnetization is possible in crystallites that are so small that it is energetically unfavorable for them to include a domain wall. An expression for the critical single-domain size is

$$d_c = 72\mu_0(A_{ex}K_1)^{1/2}/J_s^2 \qquad (18)$$

This quantity is generally less than a micrometer.

Brown's Theorem

This is an exact inequality that does not depend on an assumption of coherent reversal. The assumption is of a completely homogeneous ellipsoidal sample, for which

$$H_c \geq 2K_1/J_s - DJ_s/\mu_0 \qquad (19)$$

We have emphasized that the coercivity achieved in practice is always much less than the anisotropy field $2K_1/J_s$. Figure 11 shows the discrepancy between H_c and H_a for laboratory and commercial magnets. Experience suggests that a development process extending over many years is needed to achieve $H_c \sim 0.3H_a$ for a new permanent magnet material. The paradox posed by Brown's theorem is resolved by realizing that real magnets are never perfectly homogeneous, but include many sorts of defects and impurities that can act as nucleation sites for magnetic reversal. Nor are they ever ellipsoidal but have irregular surfaces. The scale for reversal is set by the domain wall width; the minimum nucleation volume is δ_w^3.

A summary of the intrinsic magnetic properties of the main phases used in permanent-magnet manufacture is shown in Table 3.

MAGNET PROCESSING

To achieve coercivity in a permanent magnet in practice, it is essential to inhibit the spontaneous nucleation of reverse domains due to the action of the demagnetizing field, which

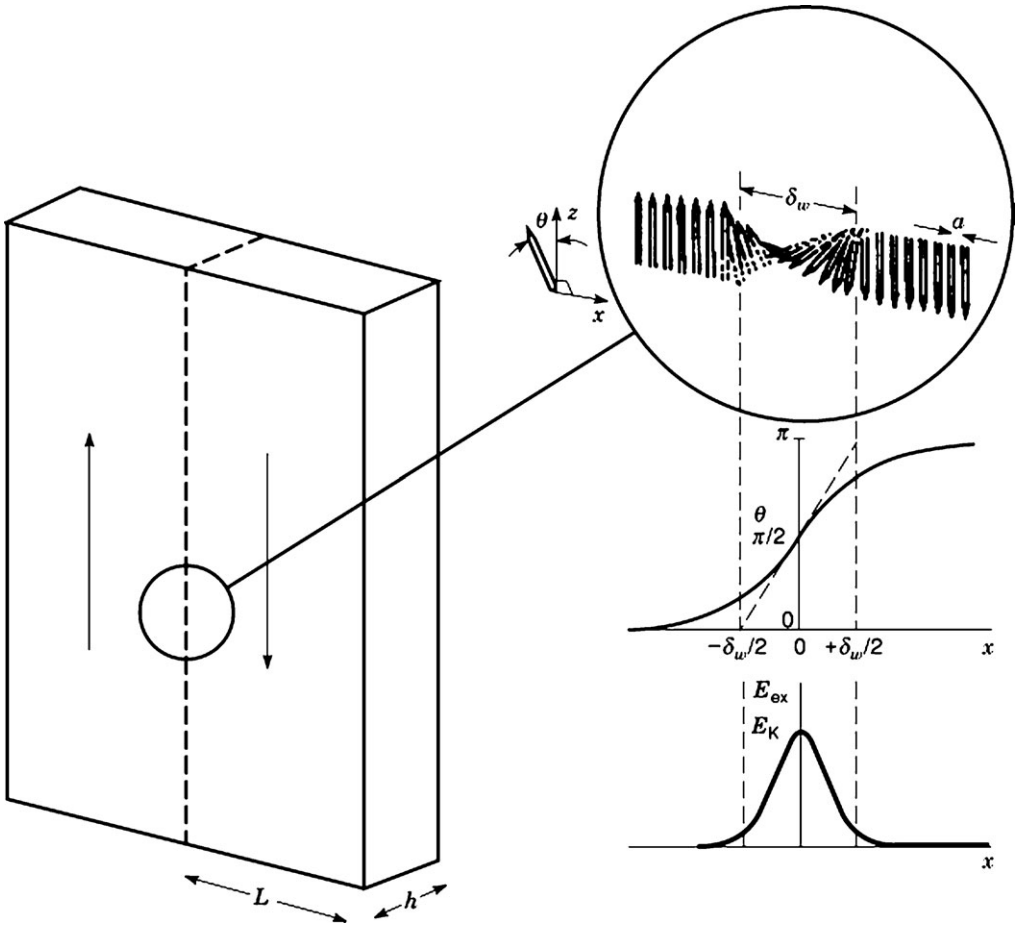

Figure 10. Schematic representation of a 180° domain wall (Bloch wall) in a material with uniaxial anisotropy. The spin configuration in the wall is shown as well as the variation in orientation and exchange or anisotropy energy across the wall.

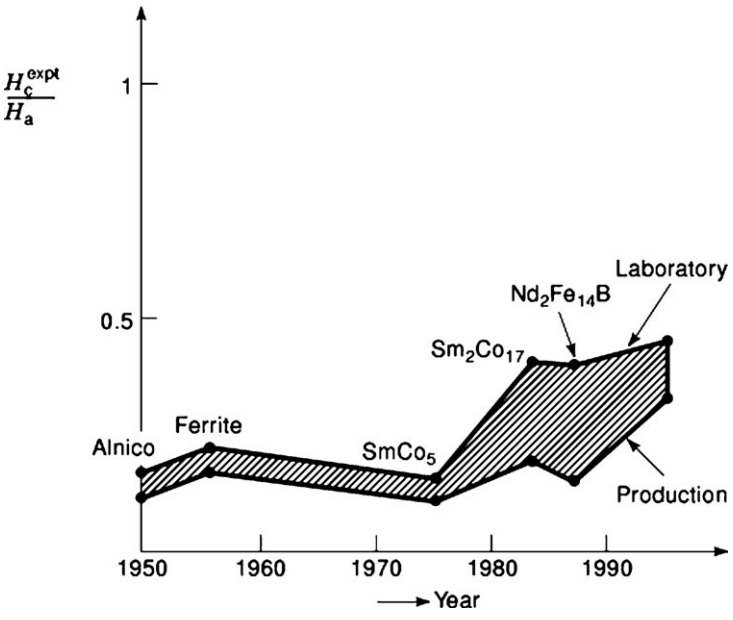

Figure 11. Illustration of the discrepancy between coercivity and anisotropy field in laboratory and production permanent magnets.

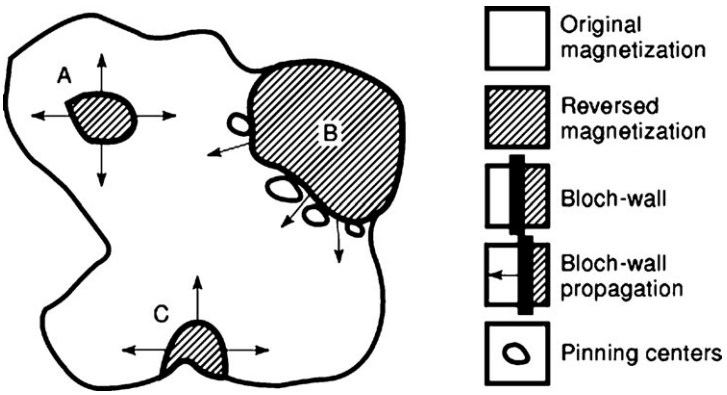

Figure 12. Overview of processes involved in magnetic reversal. *A* is a reverse domain that nucleates in the bulk from a defect or by spontaneous thermal fluctuation, *B* is a reverse domain that has grown to the point where it is trapped by pinning centers, and *C* is a reverse domain that nucleates at a rough surface.

is greatest at defects and irregularities on the surfaces of the magnetic grains. But it is also helpful to pin whatever domain walls may be present to prevent the reverse domains from growing. Pinning centers can be defects or inclusions that are comparable in size to the domain wall width. The reversal processes are shown schematically in Fig. 12.

Magnets are usually manufactured by powder metallurgical or ceramic techniques. They are therefore composed of countless tiny crystalline grains in the size range 1 μm to 10 μm. The ideal microstructure for a uniaxial material is one where the c axes of all the crystallites are aligned parallel. Remanence for this fully aligned texture can then be as high as the spontaneous polarization. If there is any misorientation of the crystallites, the local magnetization will tend to revert to the nearest c direction on decreasing field in the first quadrant. Provided there are no reverse domains,

$$J_r/J_s = \int P(\Psi)\cos\Psi\, d\Psi / \int P(\Psi)\, d\Psi \qquad (20)$$

where the function $P(\Psi)$ represents the texture of the distribution of crystallite orientations; Ψ is the angle between the c axis and the magnetizing field. When the distribution is completely *isotropic*, $P(\Psi) = \sin\Psi$ and $J_r/J_s = 0.5$.

A common type of magnet consists of randomly oriented magnetic crystallites bonded in a polymer matrix. This may be cheap to produce, but $(BH)_{max} < J_r^2/4\mu_0$ so the energy product will be less than a quarter of the value obtainable from a similar, oriented magnet. Another drawback is that only a fraction $f \approx 0.7$ of the composite is made up of magnetic grains, which dilutes the polarization and further reduces the energy product by a factor f^2. The effects of orientation and bonding on the properties of typical ferrite magnets are shown in Table 4.

Some useful microstructures for permanent magnets are shown in Fig. 13. Figure 13(a) is an array of single-crystal grains with smooth surfaces embedded in a non-magnetic matrix, which could be the polymer, or a second phase produced by suitable heat treatment of an alloy of appropriate composition. Figure 13(b) is an array of randomly oriented, submicron crystallites each of which is smaller than d_c. It can be a single-phase magnet in which a very finely divided crystalline structure is achieved by rapid quenching from the melt, hydrogen-induced disproportionation or intense cold-working, followed by annealing to crystallize the phase. Here the domains may include several crystallites and the domain walls tend to follow the grain boundaries. Figure 13(c) is a microstructure where the crystallites of the hard phase are criss-crossed by planar defects of a softer phase whose thickness is of the order of the domain wall width. The walls are then pinned at the defects and are difficult to move. Such a structure is rarely achieved because δ_w is so small. The one example concerns Sm–Co magnets. The first Sm–Co magnet consisted simply of particles of $SmCo_5$, but modern, optimized Sm–Co magnets now include three or more additional elements and exhibit a three-phase lamellar microstructure that pins the domain walls.

Microstructure is an area where theory is yet unable to offer a comprehensive guide to action. It remains the domain of art and jealously guarded commercial secrecy. A fabrication process that yields fine magnets in one environment may not be readily transplanted to another.

A general summary of the process steps involved in producing different types of permanent magnets is given in Fig. 14.

MAGNET MATERIALS

Alnico

Alnico magnets are a family of Fe–Co–Ni–Al alloys with possible additions of Cu, Ti, etc. There are two main groups, isotropic alloys with 0 wt % to 20 wt % Co and anisotropic alloys with 22 wt % to 40 wt % Co. Complex heat treatments are needed to generate the intricate metallurgical microstructure by spinodal decomposition, which is required to generate shape anisotropy associated with elongated Fe–Co regions, which may be 120 nm long and 15 nm in diameter. The anisotropic compositions, such as Alnico 5, are cooled from about 1200°C in a magnetic field.

The Alnico compounds offer moderate magnetic performance. Coercivity is limited to about 100 kA/m, and the energy product in industrial magnets is around 40 kJ/m^3, although values over 100 kJ/m^3 have been attained in the laboratory. The remanent polarization can be as high as 1.4 T. Alnicos were widely used for general-purpose applications in the middle of the twentieth century, but have been largely superseded by hexagonal ferrite and rare-earth magnets. Uncertainty in the supply and price of cobalt contributed to their relative decline. Now they are mainly confined to niche applications such as watt-hour meters

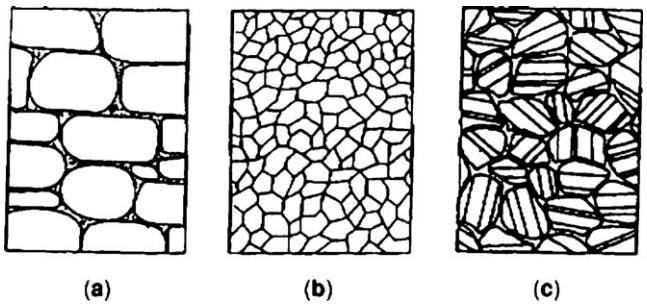

Figure 13. Some ideal microstructures for permanent magnets.

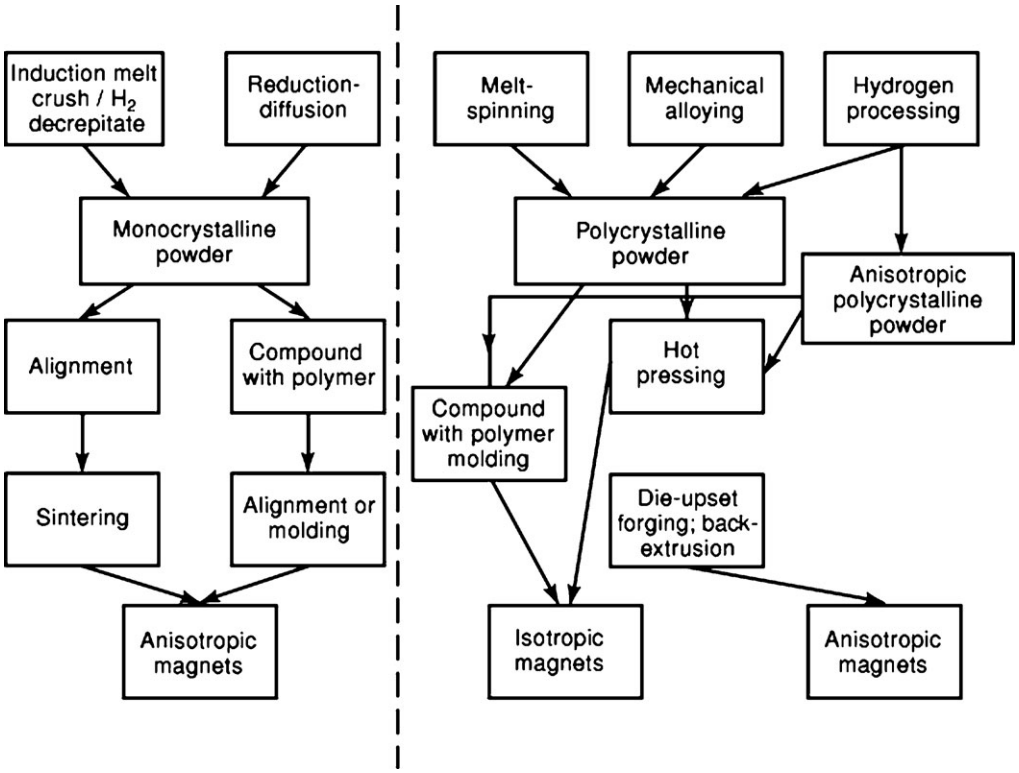

Figure 14. Overview of permanent-magnet processing. Sintering and hot pressing are not applicable to $Sm_2Fe_{17}N_3$. The anisotropic polycrystalline powder refers to $Nd_2Fe_{14}B$ only.

requiring high thermal stability or high-temperature applications where a high Curie temperature is essential.

Ferrite

The ferrites most useful as permanent magnets have the hexagonal magnetoplumbite structure (M-ferrites). The best materials are $BaFe_{12}O_{19}$ and $SrFe_{12}O_{19}$. Many chemical substitutions are possible in the structure, but few of them improve the permanent-magnet properties. All the magnetic cations are Fe^{3+}, with an atomic moment of 5 μ_B. There are five different iron sites in the structure, and the moments of the iron on three of them (eight ions/formula) are coupled antiparallel to the other two (four ions/formula). This leads to a net moment of 20 μ_B/formula, which is observed at low temperature. The Curie temperature is 470°C, and the room temperature polarization, J_s = 0.46 T, is low compared to that of other magnets. However, ferrites have the advantage in that they are cheap and easy to produce. They are manufactured in huge quantities, of the order of 1 million tonnes/year, and represent 55% of the entire permanent magnet market.

The anisotropy in hexagonal ferrites is of magnetocrystalline origin, arising mainly from one of the ferric ions, which is in a site with very asymmetric fivefold oxygen coordination. The anisotropy field is a factor of 4 or 5 greater than the magnetization, which makes it feasable to develop the coercivity required to make permanent magnets of any shape. There is an unusual temperature dependence of coercivity, with a maximum at about 220°C, which reflects the sum of different sublattice contributions to the anisotropy field.

Sintered or bonded ferrite magnets are made from monocrystaline powder prepared from Fe_2O_3 and $BaCO_3$ or $SrCO_3$ precursors having a particle size of order 1 μm to 2 μm. Since the critical single domain size d_c is 0.9 μm, the powder is generally multidomain in the unmagnetized

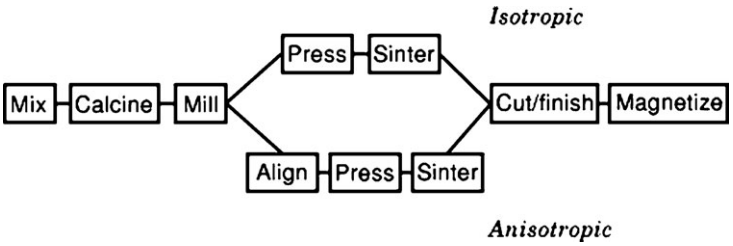

Figure 15. Steps involved in processing ferrite permanent magnets.

state. In sintered ferrites, the crystallites may be oriented as a green compact before pressing and firing at 1200°C to 1250°C to give a highly dense ($f > 95\%$) ceramic. Magnetization requires an applied field of 1.0 T to 1.5 T, about three times the coercivity. Processing steps for isotropic and anisotropic (oriented) ferrite magnets are summarized in Fig. 15.

A different route is taken for polymer-bonded magnets. Coercive powder, with a particle size of about 1 μm, is compounded with a thermoplastic, thermosetting, or rubber agent. The mixture may be molded, die-pressed, extruded, or rolled to give the desired shape. Properties of differently processed ferrite magnets were compared in Table 4.

Sm-Co

The first generation of rare-earth permanent magnets were binary alloys of cobalt and samarium having the hexagonal $CaCu_5$ structure. The basic idea of using 4*f*-3*d* intermetallics is to combine the best features of both components. The rare-earth atoms offer strong uniaxial magnetocrystalline anisotropy when they occupy sites of appropriate symmetry. The 3*d* atoms iron and cobalt combine a large magnetization with a useful Curie temperature. When these attributes are preserved in the compound, a useful permanent magnet is possible. $SmCo_5$ has a huge anisotropy field, over 30 MA/m, which makes the development of coercivity rather easy. Monocrystalline powder can be aligned and sintered or bonded to give nucleation-type magnets, like the hexagonal ferrites.

The related Sm–Co alloy with the rhombohedral Th_2Zn_{17} structure has insufficient anisotropy to permit the achievement of high coercivity, but a second generation of Sm–Co based magnets with composition $Sm(Co, Fe, Cu, Zr)_x$ with $x = 7.2$ to 8.5 was developed in the 1970s with composition intermediate between 1 : 5 and 2 : 17 wherein there is extensive chemical substitution of Fe, Cu, and Zr for Co. Fe helps to increase the polarization and reduce the cost, whereas Cu and Zr serve to refine the microstructure. (Cobalt is roughly 100 times as expensive as iron, comparable in cost to the light rare earths Sm or Nd.) These alloys show a nanoscale intergrowth of the two structure types that leads to coercivity by domain-wall pinning.

Samarium–cobalt magnets all exhibit high Curie temperatures, and the temperature dependence of the magnetization can be reduced to a negligible value by substituting some heavy rare earth such as gadolinium for samarium. These features guarantee that Sm–Co magnets will continue to find applications where elevated temperatures, up to 300°C, are involved or when a highly stable magnetic field is required in an environment of varying temperature.

Nd-Fe-B

The discovery of the tetragonal $Nd_2Fe_{14}B$ phase in 1983 marked a turning point in permanent magnetism. A potentially inexpensive, iron-based material with magnetic properties superior to any of its predecessors was rapidly developed because it was possible to adapt the techniques of powder metallurgy already in place for Sm–Co to make sintered magnets. A novel alternative processing route involving rapid quenching from the melt was also launched to produce coercive nanostructured powder suitable for polymer bonding. Many variants of these two processing routes now exist. Numerous additives such as Dy, Co, Ga, etc., can be used to tune the magnetic properties. There is now a wide range of grades of sintered magnets and coercive powder on the market. Remanent polarization can be as high as 1.5 T, and coercivity can exceed 2 MA/m.

Nd–Fe–B magnets hold the record for energy product (450 kJ/m^3) and the value of the annual production ($2.0 billion in 2005) rivals that of ferrite. In terms of cost per unit of magnetic energy, roughly $1 per joule, the two are comparable. Despite the weak points of a rather low Curie point and susceptibility to corrosion, Nd–Fe–B magnets have found myriad uses, displacing Sm–Co in some cases and opening the way to many new products including very thin voice-coil actuators for computer disk drives.

The magnetocrystalline anisotropy arises mostly from the two Nd sites in the tetragonal structure, but there is also some contribution from the iron sites. The Nd and Fe sublattices are aligned parallel producing a room-temperature polarization of 1.61 T in the pure phase, the largest of any rare-earth intermetallic that can be used for permanent magnets.

The critical single-domain size for $Nd_2Fe_{14}B$ is $d_c = 0.24$ μm, whereas the domain wall width is $\delta_w = 4.2$ nm. The walls move freely across the crystallites in an applied field as the virgin sample is magnetized to saturation. The coercivity depends on the ability of the crystallites to resist nucleation and growth of reverse domains in a reversed magnetic field. This is more difficult to achieve in $Nd_2Fe_{14}B$ than in $SmCo_5$ because the anisotropy field is five times smaller.

Fortunately, the ternary Nd–Fe–B phase diagram is suitable for realizing a coercive microstructure. Originally, the optimum composition for sintered magnets was found to be $Nd_{15}Fe_{77}B_8$, which is both Nd- and B-rich with respect to the stoichiometric $Nd_{12}Fe_{82}B_6$ composition. This falls in a region where three phases coexist at 1050°C : $Nd_2Fe_{14}B$, $NdFe_4B_4$, and a Nd-rich liquid. The latter are both nonmagnetic phases, and the Nd-rich liquid promotes liquid-phase sintering where the $Nd_2Fe_{14}B$ grains are wetted by

a surrounding liquid film, giving a microstructure like that shown in Fig. 13(a). The surfaces of the hard magnetic grains are smooth, and intergrain interactions are negligible so the microstructure tends to prevent nucleation of reversed domains and the propagation of reversal from grain to grain. The ideal two-phase microstructure in an Nd–Fe–B sintered magnet consists of fully aligned grains of $Nd_2Fe_{14}B$ separated by the minimum amount of a nonmagnetic intergranular phase. The best commercial magnets approach this ideal.

A different microstructure and magnetization process is encountered in nanocrystalline Nd–Fe–B magnets produced by melt-spinning or hydrogen processing. These processes usually yield material composed of tiny crystallites with an isotropic distribution of c-axis orientation, although some methods exist for texturing the material to make it anisotropic so that the easy axes becomes partly aligned. The initial magnetization process is relatively difficult as the domain walls tend to be trapped at the boundaries between the crystallites. The remanent state is composed of multigrain domains composed of groups of crystallites where the c axis lies in roughly the same direction. Magnetization reversal is rather extended in field, proceeding by nucleation and growth of reverse domains as in sintered magnets. The pseudodomains with the greatest misorientation to the applied field tend to reverse last.

Fitting the phenomenological expression for generalized single-domain behavior, Eq. (17), to data on sintered Nd–Fe–B magnets yields $\alpha \approx 0.4$ and $D_{\text{eff}} \approx 1$, whereas the data on melt-spun Nd–Fe–B magnets yields $\alpha \approx 0.8$ and $D_{\text{eff}} \approx 0.8$. The reduction in N_{eff} may be ascribed to the more regular crystallite shapes in the melt-spun material. A microscopic model for the coercivity in nucleation-type magnets relates the process to magnetization reversal in a critical volume. This activation volume, which can be deduced from an analysis of magnetic viscosity, is a small multiple of δ_w^3.

Sm-Fe-N

The magnetic properties of rhombohedral Sm_2Fe_{17} are completely unsuitable for permanent magnets; it has a Curie temperature of only 115°C, and the anisotropy constant K_1 has the wrong sign. However, by introducing nitrogen into the structure from a gas atmosphere, the properties are transformed. The structure is preserved, with a 6% increase in volume, but the Curie temperature rises to 475°C, and the crystal field created by the three nitrogen atoms that surround the Sm site in $Sm_2Fe_{17}N_3$ leads to an anisotropy field of 11 MA/m, which is quite sufficient to develop coercivity. The saturation polarization is a little less than that of $Nd_2Fe_{14}B$ (Table 3). The compound is metastable, and the powder cannot be sintered to produce dense oriented magnets. It is most useful for anisotropic polymer-bonded magnets. An analagous compound with carbon has somewhat inferior properties.

Other Materials

Other magnets used for niche applications include tetragonal CoPt and FePt, which have an ordered fcc structure. There is strong easy-axis anisotropy, but no unique c axis in a macroscopic specimen because the tetragonal crystallites can grow along any of the three cube edges. Isotropic magnets with remanent polarization 0.65 T, coercivity 360 kA/m, and energy products of 75 kJ/m^3 can be obtained.

Cobalt itself can be used as a magnet in thin-film devices. Although the hexagonal phase has an anisotropy constant of only 400 kJ/m^3, additives such as Cr and Ta allow the development of an in-plane texture that avoids the demagnetizing field. Magnetized cobalt films can then be used to create a small bias field on an adjacent magnetic layer, as in some magnetoresistive read heads for magnetic recording. Cobalt-based films are also used as recording media on hard disks.

MAGNET APPLICATIONS

The unique feature of permanent magnets is their indefinite ability to deliver magnetic flux into the air gap with no continuous expenditure of energy. The main applications classified in Table 2 are now considered in more detail.

A steady homogeneous field may be used to generate torque Γ or align existing magnetic moments $\boldsymbol{m}$ since $\Gamma = \boldsymbol{m} \times \boldsymbol{B}$. The corresponding quantum phenomenon is Zeeman splitting of atomic or nuclear energy levels. Charged particles of charge q moving through the uniform field with velocity $\boldsymbol{v}$ are deflected by the Lorentz force $\boldsymbol{F} = q\boldsymbol{v} \times \boldsymbol{B}$, which causes them to move in a helix in free space with the cyclotron frequency $f_c = eB/2\pi m$, which is 28 GHz/T for an electron. When the electrons are confined to a conductor of length L aligned perpendicular to the field where they constitute a current I, the Lorentz force leads to the familiar expression $F = BIL$. Conversely, moving a conductor through the field produces an induced emf given by Faraday's law $\mathscr{E} = -d\Phi/dt$, where Φ is the flux threading the circuit of which the conductor forms a part.

Spatially inhomogeneous fields offer another series of potentially useful effects. They exert a force on a magnetic moment given by the energy gradient $\mathrm{F} = -\nabla(\boldsymbol{m} \cdot \boldsymbol{B})$. They also exert nonuniform forces on charged particles, which can be used to focus ion or electron beams or to generate electromagnetic radiation as electron beams pass through the inhomogeneous field. The ability of rare-earth permanent magnets to generate complex flux patterns with rapid spatial variation ($|\nabla \boldsymbol{B}| > 100$ T/m) is unsurpassed by any electromagnetic device. This point can be appreciated by considering the Amperian surface current equivalent to a long magnet with $\boldsymbol{J} \approx 1$ T, which is about 800 kA/m. Solenoids, whether resistive or superconducting, would need to be several centimeters in diameter to accommodate the requisite ampere-turns. Permanent magnet structures can be produced by assembling blocks of rare-earth or ferrite magnets in any desired orientation. The field of one magnet does not significantly perturb the magnetization of its neighbors because the longitudinal susceptibility is zero for a square hysteresis loop, and the transverse susceptibility M_s/H_a is only of order 0.1 since the anisotropy field H_a is much greater than the magnetization (Table 3). Hence, for example, the directions of magnetization of two blocks of $SmCo_5$ in contact, with their easy directions perpendicular, will deviate by less than a degree from the easy

directions. A consequence of the rigidity of the magnetization is that the superposition of the induction of rare-earth permanent magnets is linear and the magnetic material is effectively transparent, behaving like vacuum with permeability μ_0. Transparency and rigidity of the magnetization greatly simplify the design of magnetic circuits.

Time-varying fields can be produced by displacing or rotating the magnets. They may induce an emf and exert forces on the resulting eddy currents in a conductor. Otherwise they may be used to switch on or sustain the other effects of a field, inducing moments in a magnetization measurement, for example.

Viewed from the standpoint of the permanent magnet, the applications are classified as static or dynamic according to whether the working point of the magnet in the second quadrant of the hysteresis loop is fixed or moving. Its position depends on the magnitude of the H field to which the magnet is subjected, which depends in turn on the shape of the magnet, the air gap, and the fields generated by electric currents flowing in the vicinity. The working point should be close to the $(BH)_{max}$ point. It will change whenever magnets move relative to each other, when the air gap changes, or if there are time-varying currents. In the first cases there is mechanical recoil, as the working point moves along the loop whereas in the latter case the recoil is active (Fig. 16). Because of their square loops, oriented ferrite and rare-earth magnets are particularly well suited for dynamic applications that involve changing flux density in the permanent magnet. Ferrites and bonded metallic magnets also minimize eddy-current losses. For mechanical recoil, the air gap changes during operation from a narrow one with reluctance R_1 to a wider one with reluctance R_2, as shown in Fig. 16(b). ($R = Hl_m/B$, where l_m is the length of the magnet.)

Active recoil occurs in permanent-magnet motors and other devices where the magnets are subject to an H field, H_{app}, during operation as a result of currents in the copper windings. The field is greatest at start-up, or in the stalled condition. Active recoil is represented by a displacement of the reluctance line along the H axis [Fig. 16(c)]. Provided $\mu_0 H_c$ exceeds B_r, it is possible to drive the working point momentarily into the third quadrant of the $B:H$ loop without demagnetizing the permanent magnet. The intrinsic coercivity may be as important a figure of merit as $(BH)_{max}$ in this type of application.

The magnets in electric machines can be subject to temperatures in excess of 100°C. Magnetization and coercivity naturally decline as the Curie point is approached, and the temperature coefficients of these quantities around ambient temperature are listed in Table 5 for magnets made of different materials. Not all the loss is necessarily recoverable on returning to ambient temperature. The maximum temperatures at which the materials can safely be used are also indicated in the table. The limit for $Nd_2Fe_{14}B$ is lower than for any of the others because of the relatively low Curie point and the temperature coefficients are more severe. These are difficulties to be overcome by astute engineering design.

An overview of rare-earth permanent magnet applications is given in Fig. 17. Details of specific applications follow.

Flux Sources

Uniform Fields. The magnetic field produced by a point dipole of moment m A · m^2 is quite inhomogeneous. In polar coordinates it is

$$H_r = 2m\cos\theta/4\pi r^3, \qquad H_\theta = m\sin\theta/4\pi r^3, \qquad H_\phi = 0 \quad (21)$$

so the magnitude and direction of H both depend on r. The field due to an extended line dipole of moment λ A · m is distinctly different:

$$H_r = \lambda\cos\theta/2\pi r^2, \qquad H_\theta = \lambda\sin\theta/2\pi r^2, \qquad H_\phi = 0 \quad (22)$$

so the magnitude of $\boldsymbol{H}$, $(H_r^2 + H_\theta^2 + H_\phi^2)^{1/2}$, is actually independent of θ; its direction makes an angle 2θ with the orientation of the magnet.

By using long segmented cylindrical magnets with a hollow bore it is possible to create a field that is uniform within a certain region of space. Choosing the orientation of each segment appropriately, the fields will all add at the center. In the transverse field design shown in Fig. 18(a), the outer surface will be an equipotential provided $t/r = \sqrt{2} - 1$, in which case the flux density in the air gap is $0.293B_r$. Multiples of this field can be obtained by nesting similar structures inside each other. Shimming to compensate any imperfections in the magnets or assembly is possible by placing appropriate compensating dipoles in the corners. Open cylinders or permanent magnets with iron yokes providing highly homogeneous fields may be used for magnetic resonance imaging. Proton images from ^{1}H nuclei are generally used for noninvasive medical imaging, but ^{31}P and ^{13}C are also feasible. The distribution of spin–lattice and spin–spin relaxation time can be mapped and specific regions highlighted by means of magnetopharmaceutical agents. Permanent-magnet flux sources supply fields of order 0.3 T in a whole-body scanner. Fields are lower than those of competing superconducting solenoids, but there is no need for any cryogenic installation. Nuclear magnetic resonance spectrometers with permanent magnet flux sources may be used for quality control in the food, polymer, and construction industries.

Figure 18(c) shows a different design where the direction of magnetization of any segment is at 2θ from the vertical axis. According to Eq. (22), all segments now contribute to create a uniform field across the air gap in the vertical direction. Unlike the structure of Fig. 18(a), the radii r_1 and r_2 can take any values without creating a stray field outside the cylinder. The device is known as a Halbach cylinder. The flux density in the air gap is

$$B = B_r \ln(r_2/r_1) \quad (23)$$

where r_1 and r_2 are the inner and outer radii. In practice it is convenient to assemble the device from n trapezoidal segments, as illustrated in Fig. 18(d) for $n = 8$. In that case, an extra factor $[\sin(2\pi/n)]/(2\pi/n)$ is included on the right-hand side of Eq. (23). The cylinders are never infinitely long; the length is typically comparable to the diameter, so the field is reduced by another factor $f(z)$, where z is the distance from the center. For example, the flux density at the center of an octagonal cylinder with r_1 = 12 mm, r_2 = 40 mm, and length 80 mm made of a grade of Nd–Fe–B

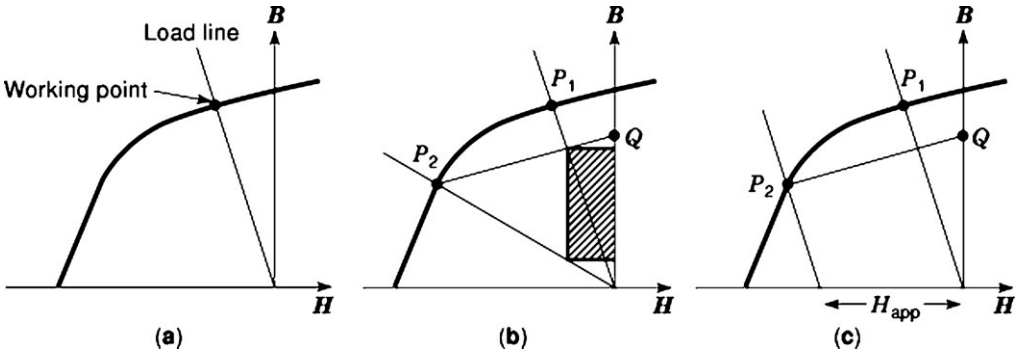

Figure 16. Hysteresis loops showing the working point for (a) a static application, (b) a dynamic application with mechanical recoil, and (c) a dynamic application with active recoil.

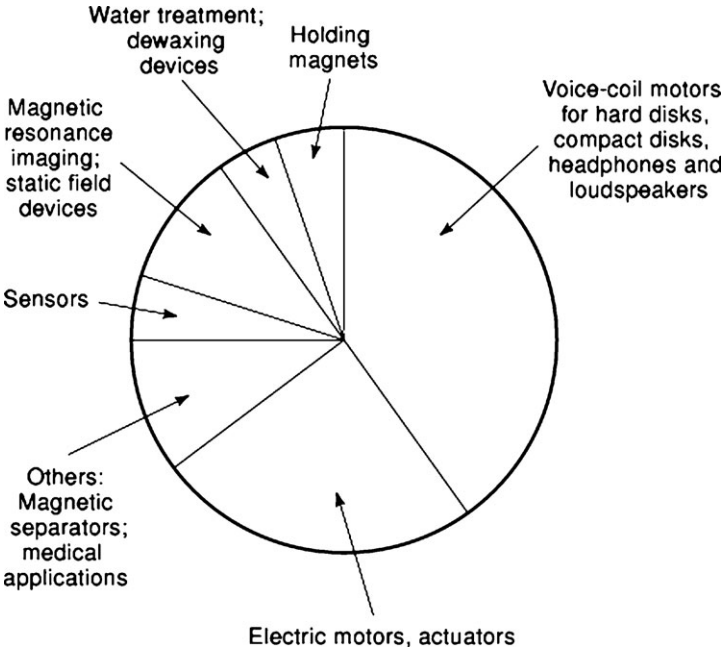

Figure 17. Overview of industrial applications of rare-earth permanent magnets.

having B_r = 1.20 T is 1.25 T, compared to the value of 1.44 T calculated from Eq. (23). Here the flux in the air gap exceeds the remanence in a circuit that uses no iron, which illustrates the principle of magnetic flux concentration.

Inhomogeneous Fields. The cylindrical configurations of Fig. 18 may be modified to produce a variety of inhomogeneous fields such as quadrupole fields, particularly useful for charged-particle beam control. Higher multipole fields than dipole are obtained by having the orientation of the magnets in the ring vary as $[(n/2) + 1]\theta$, where $n = 2$ for a dipole field, $n = 4$ for a quadrupole, and so on. The design of Fig. 18(e) produces a quadrupole field. The field at the center of the quadrupole is zero, but whenever the particle beam deviates it experiences an increasing field that causes its trajectory to curve back to the center. Multipole rings known as magnetrons are used in sputtering systems to increase the ionization of the plasma near the target by extending the paths of the electrons into helices around the field lines. The magnets in an ion pump have a similar function. Magnetrons in domestic microwave ovens are devices in which electrons emit cyclotron radiation as they move in trajectories determined by the field of a ferrite ring magnet.

Other arrangements of cylindrical magnets produce a uniform magnetic field gradient along a particular direction. Field gradients are especially useful for exerting forces on other magnets.

Another type of permanent-magnet structure creates an inhomogeneous magnetic field along the axis of the magnet, which is the direction of motion of a charged-particle beam. Microwave power tubes such as the traveling-wave tube are designed to keep the electrons moving in a narrow beam over the length of the tube and focusing them at the end while coupling energy from an external helical coil. Originally this was achieved by applying a uniform axial field from a resistive solenoid, but the design with permanent-magnet focusing by a periodic axial field in Fig. 19(a) is just as effective and represents a great saving in weight and power when $SmCo_5$ magnets are used.

Insertion devices for generating intense beams of hard radiation (UV and X ray) from energetic electron beams in synchroton sources use a periodic transverse field. These devices are known as wigglers, since they cause the elec-

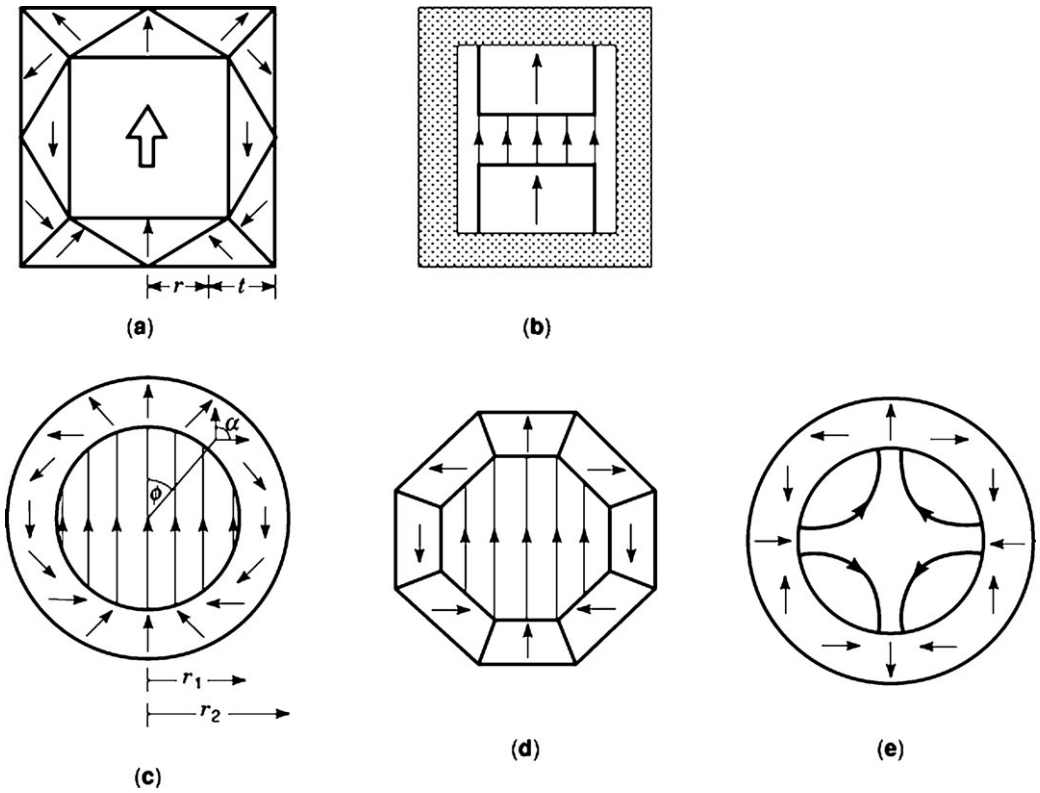

Figure 18. (a–d) Cross-sections of some permanent-magnet structures that produce a uniform transverse field. The shaded material in (b) is a soft-iron yoke. (e) produces a quadrupole field.

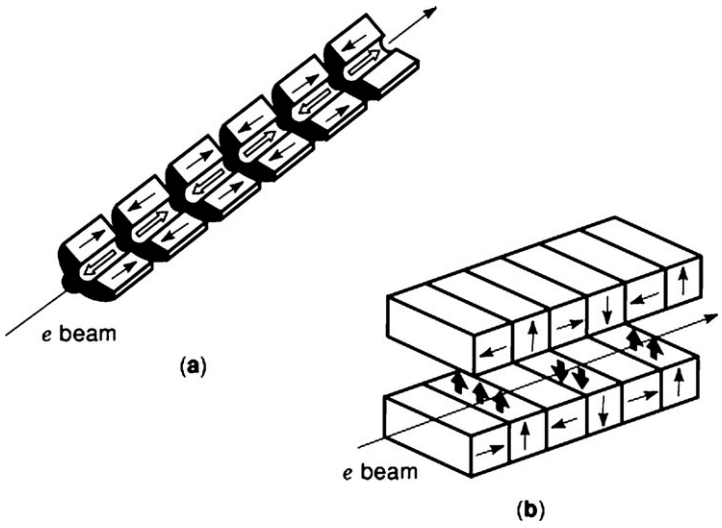

Figure 19. Periodic flux sources: (a) a magnet for a microwave traveling-wave tube; (b) a wiggler magnet used to generate intense electromagnetic radiation from an electron beam.

trons to travel in a sinuous path. Similar structures are used in free-electron lasers. A design that includes segments magnetized in a parallel direction to concentrate the flux is shown in Fig. 19(b).

Simple force applications in catches and closures consume large amounts of sintered ferrite. Bonded ferrite magnetized in strips of alternating polarity is widely used for fixing signs and light objects to steel panels.

Variable Fields. Fields can be varied by changing the air gap or by some movement of the magnets in a structure with respect to each other. The working point is displaced as the magnets move so these devices involve mechanical recoil. A simple type of variable flux source is a switchable magnet. These are often used in holding devices, where a strong force is exerted on a piece of ferrous metal in contact with the magnet. The working point shifts from the open circuit point to the remanence point where $H = 0$ as the circuit is closed. The maximum force F that can be exerted at the face of a magnet of area A_m where the flux density

is B_m is given by

$$F/A_m = B_m^2/2\mu_0 \qquad (24)$$

Forces of up to 40 N/cm^2 can be achieved for B_m = 1 T.

To create a uniform variable field, two Halbach cylinders of the type shown in Fig. 18(d) with the same radius can be nested inside each other. Then by rotating them through an angle $\pm\alpha$ about their common axis, a variable field 2 cos α B_r ln(r_2/r_1) is generated (Fig. 20(a)). Another solution is to rotate the rods in the device of Fig. 20(b). By gearing a mangle with an even number of rods so that the alternate rods rotate clockwise and anticlockwise though an angle α, the field varies as B_{max} cos α. Further simplification is possible with a magnetic mirror, a horizontal sheet of soft iron containing the axis of symmetry that produces an inverted image of the magnets and halves the number required.

These permanent-magnet variable flux sources are compact and particularly convenient to use since they can be driven by stepping or servomotors, and they have none of the high power and cooling requirements of a comparable electromagnet. For example, the flux source illustrated in Fig. 21 uses 28 kg Nd–Fe–B magnets of the design shown in Fig. 20(a) to generate fields up to 2 T in a 25 mm bore. Large rotating or alternating fields can be generated by rotating the magnets continuously.

The limit to the fields that can be generated using permanent magnets is about 5 T. This is set in part by the coercivity of the material. Half of the vertical segments in Fig. 18(a, c, and d) are subject to a reverse H field equal to the field in the bore. But there is also a practical size limitation imposed by the exponential increase in dimension of Eq. (23). Admitting a material existed with B_r = 1.5 T and $\mu_0 H_c$ = 5 T, the diameter required to achieve 5 T in a 25 mm bore is 700 mm. Such a structure 400 mm high would weigh about a ton. Permanent-magnet variable flux sources can rival resistive electromagnets to generate fields of up to about 2 T, but they cannot compete with superconducting solenoids in the higher-field range.

Couplings and Bearings

Permanent magnets are useful for coupling rotary or linear motion when no contact between members is allowed, for example, across the wall of a chamber operating in vacuum or in an aggressive environment. Figure 22 illustrates the design of a simple rotary coupling and a magnetic gear. Forces depend quadratically on the remanence of the magnets, so it is advantageous to select material with a large polarization. If the coupling slips, the magnets may be subjected to a substantial reverse field, so a high coercivity is also required. Rare-earth magnets are ideal here. The torque varies sinusoidially with the relative angular displacement of the two members of the coupling with period $4\pi/p$, where p is the number of magnetized segments. The maximum torque can be varied by adjusting the air gap. Torques of order 10 N · m may be achieved in couplings a few centimeters in dimension.

Magnetic bearings are simple, cheap, and reliable. They are best suited to high-speed rotary suspensions in flywheels or turbopumps, for example. Linear suspensions have been tested in prototype magnetically levitated transportation systems. It is a feature of magnetic bearings that a mechanical constraint (or active electromagnetic support) is generally required in one direction. Unfortunately it is impossible to design a field configuration that will draw a small magnet towards a fixed point in space. If such a point O existed, then the field at that point would have to satisfy the condition that dB/dx, dB/dy, and dB/dz are all negative, which contradicts Maxwell's equation $\nabla \cdot \boldsymbol{B}$ = 0. The impossibility of stable magnetostatic levitation of a magnet at a point using only permanent magnets in free space is known as Earnshaw's theorem. Stable levitation is possible however when diamagnetic materials are introduced.

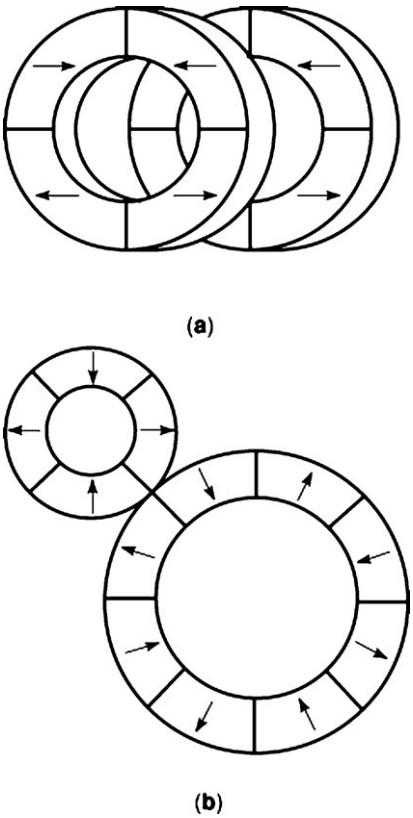

Figure 22. (a) A face-type coupling with four axially magn
with radially magnetized segments.

The simplest bearings are made of two ring-shaped magnets in repulsion. Some configurations provide a radial restoring force provided the axis is prevented from shifting or twisting. Others support a load in the axial direction but must be prevented from moving in the radial direction. The linear magnetic bearings provide levitation along a track, but lateral constraint is required. It is impracticable to equip a great length of track with permanent magnets, so instead levitation may be provided by repulsion from eddy currents generated in a track of metal plates or by attraction of the magnets on the magnetically-levitated vehicle to a suspended iron rail.

Magnetic Separation

Magnetic separation is a technology based on inhomogeneous or time-varying magnetic fields that affords great

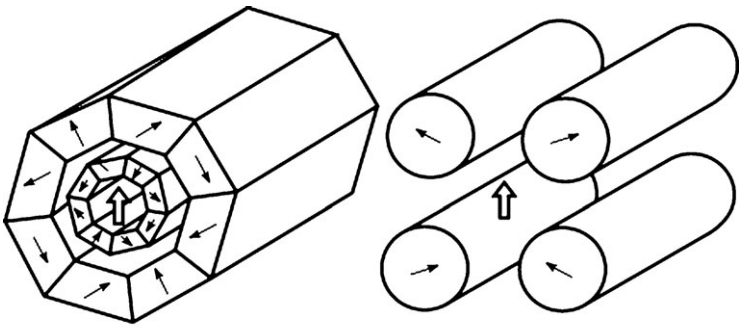

Figure 20. Permanent-magnet variable flux sources (schematic). (a) A double Halbach cylinder, (b) a four-rod "mangle."

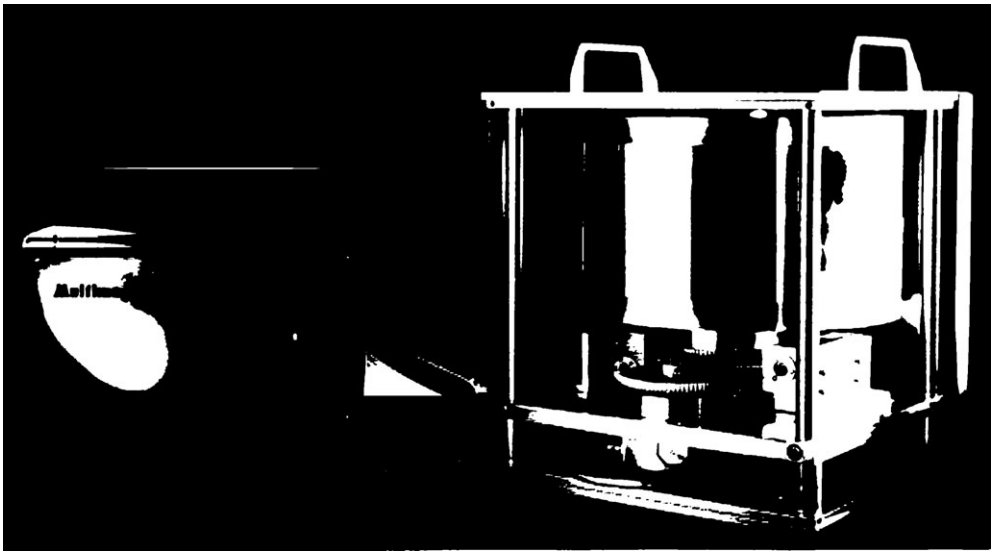

Figure 21. A 2 T variable flux source, based on the design of Fig. 20(a). (Photo by courtesy of Magnetic Solutions Ltd.)

economic and social benefits. The expression for the energy of a magnetic moment $\boldsymbol{m}$ in a field $\boldsymbol{H}$ is $-\mu_0 \boldsymbol{m} \cdot \boldsymbol{H}$, leading to the expression $F = \mu_0 \nabla(\boldsymbol{m} \cdot \boldsymbol{H})$. However, when the moment m is induced by the field in a material with susceptibility χ, the expression becomes

$$F = \tfrac{1}{2}\mu_0 \chi V \nabla(H^2) \qquad (25)$$

To separate ferrous and nonferrous scrap or to select minerals from crushed ore on the basis of their magnetic susceptibility it is sufficient to use open gradient magnetic separation in which material tumbles through a region where there is a strong magnetic field gradient. Field gradients in open gradient magnetic separators may be $\approx$10 T/m and separation forces are of order 10^7 N/m^3.

High-gradient magnetic separation is suitable for capturing weakly paramagnetic material such as red blood cells. Here a liquid containing the paramagnetic solids in suspension passes through a tube filled with a fine ferromagnetic steel mesh or steel wool, which distorts the flux pattern in an applied field, creating local field gradients as high as 10^5 T/m and separation forces can reach 10^{11} N/m^3. The paramagnetic material remains stuck to the wires until the external field is switched off, when it may be flushed out of the system. Switchable permanent magnets can be used to create the field.

A different principle is employed in electromagnetic separation to sort nonferrous metal such as aluminum cans from nonmetallic material in a stream of refuse (Fig. 23). A fast-moving conveyor belt carries the rubbish over a static or rotating drum with embedded ferrite or rare-earth magnets. The relative velocity of the magnets and the refuse may be 50 m/s. Eddy currents induced in the metal create a repulsive field, and the metal is thrown off the end of the belt in a different direction to the nonmetallic waste. In electromagnetic separation, deflection depends on the ratio of conductivity to density, so it is possible to separate different metals such as aluminum, brass, and copper.

Sensors

Magnetic sensors are based on detecting a varying field in an air gap using a Hall effect or magnetoresistance probe that delivers a voltage proportional to B (sometimes B^2). Magnetic position and speed sensors are used in automobile system controls, where they offer reliable noncontact sensing in a hostile environment involving dirt, vibration, and high temperatures. Examples are crankshaft position

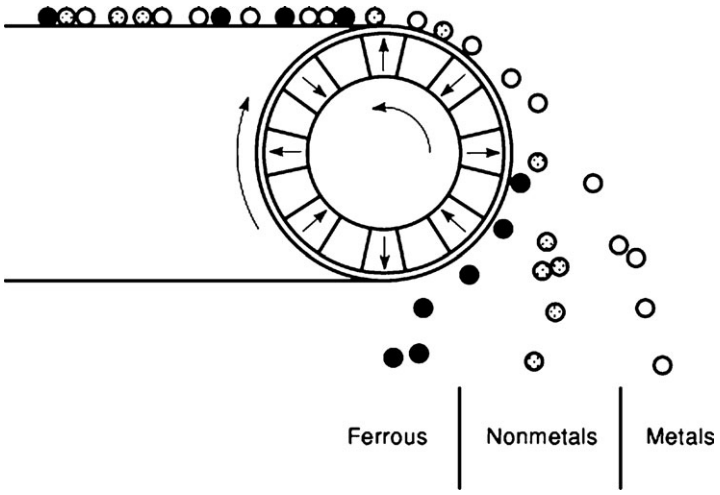

Figure 23. Electromagnetic separation with permanent magnets.

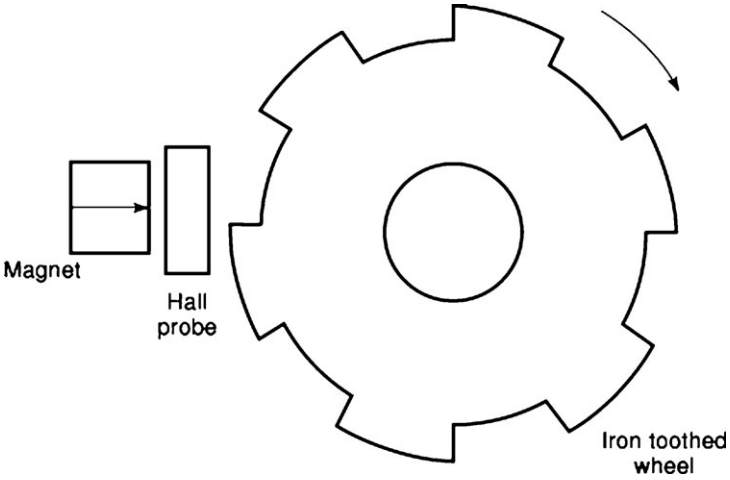

Figure 24. A variable-reluctance sensor.

sensors and sensors for automatic braking systems. The design shown in Fig. 24 is a variable-reluctance sensor where the teeth on the iron gear wheel cause a modulation of the sensor voltage as the wheel rotates. Angular position sensors built into electronically commutated motors can be simple Hall sensors that detect the stray field produced by a multipole rotor.

Motors and Actuators

Motors and actuators whose operation depends on permanent magnets are produced in huge quantities, exceeding 10^8 units/year. A household that owned three motors 50 years ago may now possess a hundred of them in domestic appliances, audio, video and computer equipment, clocks, watches, toys, and the family car. Many of these are small dc permanent magnet motors. Dc servomotors are found in machine tools, robots, and other industrial machinery. Permanent magnets can also be used to advantage in large industrial drives, bringing savings in weight, energy, and material costs. When electric vehicles become a widespread reality, yet more magnets will enter our daily lives. The ability to fabricate ferrite or rare-earth magnets in any desired shape has led to many permutations on a few basic electrical machine designs. One limitation is the maximum working temperature of high-remanence grades of Nd-Fe-B and ferrite that cannot match the running temperatures of many classical induction motors (Table 5).

An actuator is an electromechanical device with a limited linear or angular displacement. The definition encompasses loudspeakers, microphones, moving-coil meters, disk-drive head actuators, actuators for industrial robots, pneumatic pumps, car door locks, noise and vibration control using antiphase displacement, and many others. Usually, the air gap is fixed, and the dynamic working is due to the H field produced by current windings. Actuators tend to be rather simple mechanical structures delivering a force directly to move a load. Dynamic response is often a critical aspect of actuator design. Three basic configurations are moving-coil, moving-magnet, and moving-iron.

Moving-coil loudspeakers have been built with permanent magnets for over 50 years. Flux is directed into a radial air gap where the voice coil is suspended, attached to a light, rigid cone (Fig. 7). The force on the coil is proportional to the flux density in the air gap B_g, and the acoustic power varies as B_g^2, which is maximized by operating near the $(BH)_{max}$ point of the magnet. Good results are obtained when B_g exceeds about 0.5 T and the mass of the voice coil is less than 1 g. Large, flat ferrite ring magnets can be used with iron to concentrate the flux (Fig. 7). These designs are cheap but inefficient as there is much flux leakage. Stray

fields are reduced in the cylindrical magnet designs using rare-earth or alnico magnets. Moving-magnet designs are feasible using Nd-Fe-B, where the magnet is glued to the cone and a stationary drive-coil surrounds it.

A large class of voice-coil actuators are similar in principle to a loudspeaker. Cylindrical configurations are used for head positioning in computer hard-disk drives and mirror positioning in laser scanners. Rapid dynamic response is assured by the low mass of the voice-coil assembly and the low inductance of the coil in the air gap. Radially magnetized ring magnets can be used to enhance the flux density in the air gap. A planar configuration is shown in Fig. 25. Here the coil is flat, and it is attached to a lever that allows it to swing in a limited arc between two pairs of rare-earth magnets. The design is favored for the flat disk drives of portable personal computers, and it requires Nd-Fe-B with the highest possible energy product (>400 kJ/m^3). Access time at constant acceleration a is proportional to $1/\sqrt{a}$, hence to $1/\sqrt{B_g}$. High-grade Nd-Fe-B is also used in the actuators in laser compact-disk and DVD players. It is remarkable that these applications account for about 25% of Nd–Fe–B production.

Moving-magnet actuators may be of the linear or rotating variety. They offer low inertia and no flying leads. Linear reciprocating actuators with a stroke of several millimeters are used in pumps at frequencies of order 50 Hz. The operating frequency is designed to correspond to the resonant frequency of the mechanical system. Rotary actuators can be regarded as electric motors with restricted travel. Moving iron actuators likewise may be linear or rotary. In the design used for a print hammer for a dot-matrix printer the hammer spring formed part of the magnetic circuit, and in the unexcited position it was held tight against the iron, with no air gap. When a current pulse passed through the solenoid, the hammer spring out. A similar principle is used in reed switches, where two flat soft iron reeds are drawn into contact by a magnetic field. The switch can be opened by activating a solenoid to create a reverse field, or simply by moving the magnet.

A vast range of motors can be designed with magnets, their power ranging from microwatts, for wristwatch motors, to hundreds of kilowatts, for industrial drives. The high-energy product and high anisotropy of the rare-earth permanent magnets makes it possible to realize compact, low-inertia, high-torque devices—stepper motors, actuators, brushless dc motors—that are the means for electronically regulated motion control. Ferrites are produced in huge quantities for low-cost motors for consumer products, including automotive applications. Sintered Nd-Fe-B is finding increasing applications in drives and generators for electric vehicles, For example 15 million electric bicycles were produced in China in 2005.

A common dc motor design is shown in Fig. 26(a). The permanent magnet on the fixed outer section, known as the stator, creates a field at the windings of the rotor. A mechanical commutator with brushes distributes current to the windings in such a way that the torque on the rotor is always in the same sense. Conversely, the device will also function as a generator, producing an emf U if it is driven at an angular velocity ω. In a dc servomotor, the torque or the angular velocity is controlled by modifying the applied voltage. Simple velocity control is based on monitoring the back-emf U, but more sophisticated control systems use a tachogenerator (a small dc motor coupled to the drive shaft) or a precise position encoder to generate a voltage fed back to control the output power.

The motor design may be modified, as shown in Fig. 16(b), to eliminate the mechanical commutator, which is a source of wear and sparking. In the brushless dc motor, the magnets are situated on the rotor, and the armature windings, now located on the stator, are energized in an appropriate sequence by means of power electronics. Electronically commutated motors are reliable and they are particularly suited to high-speed operation, $\omega > 30$ c/s; (i.e., >1000 revolutions/minute). Position sensors form an integral part of the device since the winding to be energized depends on the position of the rotor.

By unrolling the armature, a linear motor is obtained. Flattening the rotor into a disk produces a pancake motor. The low moment of inertia means that high angular accelerations are possible, especially when Nd-Fe-B is used for the magnets. They may be embedded in the rotor so as to concentrate the air-gap flux.

A feature of all permanent-magnet motors is armature reaction. The currents in the armature, whether the armature windings are on the stator or on the rotor, create a field which is usually in a direction opposed to the magnetization. The working point of the magnets is shifted, as shown in Fig. 16(c). The effect is particularly severe at the trailing edges of the poles, and a solution is to make these sections from a high-coercivity magnet grade.

A stepping motor is a device that rotates through a fixed angle when one of the windings is energized by a suitable electronic control circuit. Stepping motors are used for precise position control. Designs may incorporate a ring magnet with many poles around the circumference. These can be fabricated from polymer-bonded ferrite by injection moulding and they are then pulse-magnetized using a special fixture. A common design of hybrid permanent-magnet stepper motor makes 200 steps per revolution, a 1.8° step size. With suitable control, it will proceed in half-steps of 0.9°. Tiny two-pole stepper motors using bonded Sm–Co magnets are used in clocks and watches.

Miscellaneous

Permanent magnet devices are extensively used in the Chinese oil industry to control the formation of paraffin wax from heavy crude in oil wells. Several magnets are inserted at different depths in the well where they create a field of about 0.1 T on the flowing oil. With the magnets in place it is claimed that the time between shutdowns to clean out the well can be increased from six weeks to six months.

A host of magnetic water treatment devices are marketed throughout the world for domestic and industrial use that serve to inhibit limescale deposits in pipework carrying hard water. They appear to influence the structure and morphology of the calcium carbonate precipitate, altering the calcite: aragonite ratio. Details are controversial. Other reports exist of a magnetic field effect on precipitation of inorganic salts from supersaturated solution,

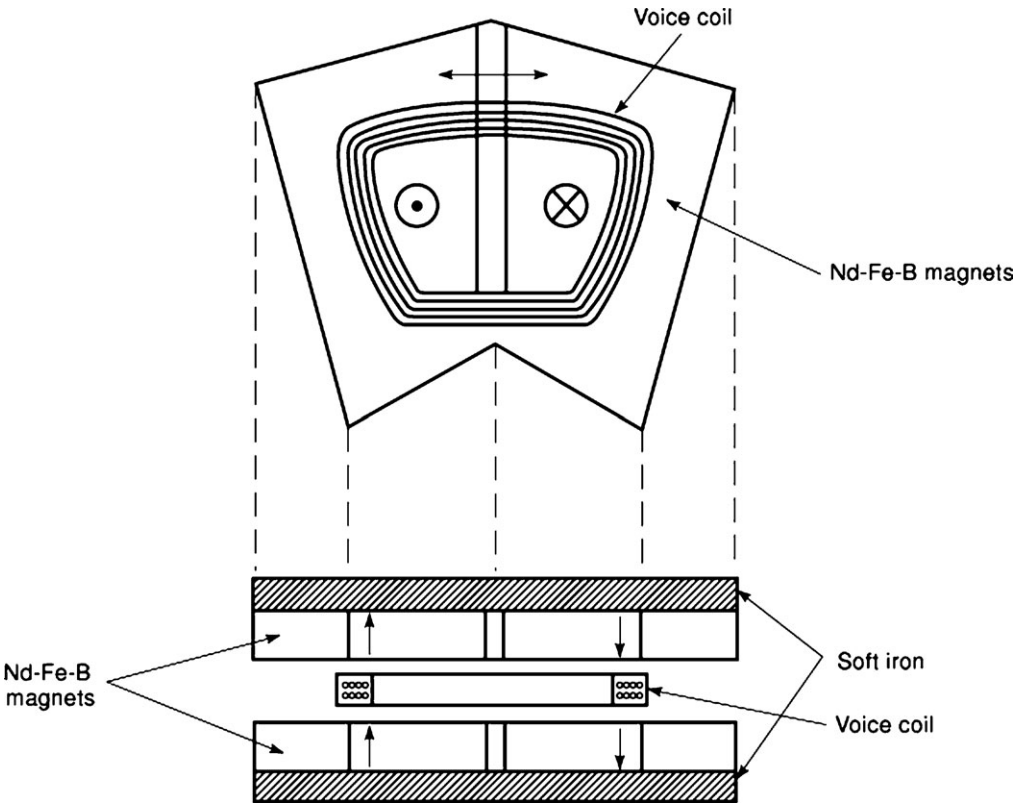

Figure 25. A flat voice-coil actuator for a personal-computer disk drive.

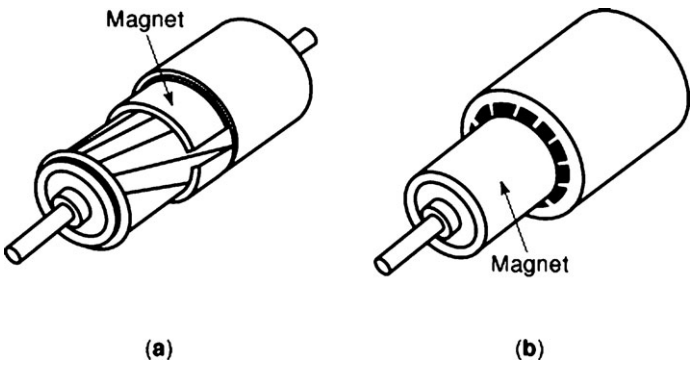

Figure 26. Dc motor designs; (a) brush motor with magnets on the stator; (b) brushless motor with magnets on the rotor.

the rate of electrodeposition of metals and electropolymerization. The reality of some of these effects seems to be in little doubt, but a convincing theory or explanation is lacking at present. If these processes were understood, it might be possible to rationally design permanent magnet devices for maximum effect in a range of industrial processes.

PROSPECTS

The burgeoning range of permanent magnet applications has been made possible by the discovery of new magnetic materials and their continual improvement. A further doubling of the energy product to 800 kJ/m^3 in due course might be possible, but redoubling to 1600 kJ/m^3 is out of the question in view of the intrinsic magnetic properties of all the materials known to be magnetically ordered at room temperature. The ferromagnet with the greatest polarization is the alloy $Fe_{65}Co_{35}$, for which J_s = 2.45 T. This sets a ceiling on $(BH)_{max}$ of 1200 kJ/m^3. The problem is to find a material with $J_s > 1.6$ T where it is possible to develop coercivity. Extensive searches for new phases have not uncovered a potentially hard magnetic material with a polarization greater than that of $Nd_2Fe_{14}B$. The best prospects for progress appear to be with nanocomposite magnets where a hard rare-earth magnet phase is compounded with a soft phase such as Fe or Fe-Co on a scale of 10 nm to 20 nm. The phases are magnetically coupled on an atomic scale, and the composite behaves as a single phase with anisotropy and polarizations which are volume averages of the two components. By using a significant fraction of Fe or $Fe_{65}Co_{35}$ it might be possible to exceed 500 kJ/m^3.

In some areas the utility of modern permanent magnets has been slow to be appreciated. There are good prospects for innovative applications. One prediction is that the elec-

tromagnet is obsolete, and likely to be superseded for many purposes by permanent-magnet variable flux sources, such as that illustrated in Fig. 21, which have great advantages of compactness and independence of large power supplies or cooling requirements.

New products such as cordless electric tools or personal stereos owe their existence to advanced permanent magnets. One may expect that other new consumer products will appear that exploit their benefits. The market is not so much vulnerable to changes in the shape of personal computers and home electronics as it is capable of great expansion as a few more mass applications emerge. The electric automobile is one of the products that could transform the scale of industrial applications of permanent magnets. Electric bicycles for the Chinese market already absorb about 15% of the sintered Nd-Fe-B produced.

Much of the future progress in permanent magnets is likely to be in the direction of more versatile and cost-effective grades, with better thermal characteristics or ease of fabrication or magnetization, for example. Bonded magnets will continue to increase their share of the industrial market. The energy product shown in Fig. 1, however, seems set to follow an S-shaped curve which fitted, more or less, into the twentieth century.

BIBLIOGRAPHY

K. H. J. Buschow, Magnetism and processing of permanent magnet materials, inK. H. J. Buschow (ed.), *Ferromagnetic Materials*, Amsterdam: North Holland, 1997, p. 463.

P. Campbell, *Permanent Magnet Materials and Their Application*, London: Cambridge Univ. Press, 1994.

J. M. D. Coey (ed.), *Rare-Earth Iron Permanent Magnets*, New York: Oxford Univ. Press, 1996.

K. J. Strnat, Modern permanent magnets for applications in electrotechnology, *Proc. IEEE*, **78**: 923–926, 1990.

J. F. Herbst, $R_2Fe_{14}B$ materials, intrinsic properties and technological applications, *Rev. Mod. Phys.*, **63**: 819–898, 1991.

R. J. Parker, *Advances in Permanent Magnetism*, New York: Wiley, 1990.

R. Skomski and J. M. D. Coey, *Introduction to Permanent Magnetism*, London: Inst. of Phys., 1999.

J. M. D. COEY
Trinity College, Dublin, Ireland